Tearing down the wall – The inclining experiment

Kristian Bertheussen Karolius*, Dracos Vassalos

Maritime Safety Research Centre, Department of Naval Architecture, Ocean and Marine Engineering, University of Strathclyde, Glasgow, Scotland, UK

This research did not receive any specific grant from funding agencies in the public, commercial, or not-for-profit sectors.

*Corresponding author. E-mail address: kristian.karolius@strath.ac.uk (K.B. Karolius)

Abstract

It is a well-known fact that the current method for calculating a ship's vertical centre of gravity (VCG) following inclining experiments is limited when considering magnitude of applied heel angle and accuracy achieved for certain hull-forms due to the assumption of unchanged metacentre position when the vessel is heeled. New methods for calculating the VCG have been proposed, notably the *Generalised* and the *Graphical* methods. This paper aims to test these methods on a range of vessels, as well as present and contrast a new method named, the *Polar* method. The test will establish the error potential for each method using a purely technical software-simulated inclining experiment. Using the established error potential, a corrected VCG is calculated from actual inclining VCG values, which have been evaluated against the loading conditions for each vessel to see if the stability margins have been compromised. The study confirms the *Classical* method's dependency on applied heel angle magnitude, the change in waterplane area and that it compromises safety in some cases. The other methods, especially the *Generalised* and the *Polar*, produce very accurate results for any floating position of the vessel, highlighting the need to *tear down the wall*-sided assumption implicit in the *Classical* method and replace it with the better and more flexible methods.

Keywords

Inclining experiment, Lightweight VCG, Calculation methods, Error potential, Ship stability, Ship safety

Nomenclature

w	inclining weight	[tonnes]
Δ	weight of displacement	[tonnes]
B_M	buoyancy mass	[tonnes]
WPA	waterplane area	[m^2]
∇	volume of displacement	[m^3]
I_{XX}	second moment of waterplane area	[m^4]
φ	heel angle	[degrees]
φ_0	initial heel angle	[degrees]
φ_i	heel angle for individual weight shifts	[degrees]
G	centre of gravity	[cx, cy, cz / m]
B	centre of buoyancy	[cx, cy, cz / m]
M	metacentre position	[cx, cy, cz / m]
M_0	metacentre position for small heel angles	[cx, cy, cz / m]
$M(\varphi)$	metacentre position for large heel angles	[cx, cy, cz / m]
M_Y	transverse heeling moment	[tonnes · m]
H_{mom}	heeling moment	[tonnes · m]
R_{mom}	righting moment	[tonnes · m]
FSM	free surface moment	[tonnes · m]
MCT	moment to change trim	[tonnes · m/cm]
R_{slope}	regression slope	[Δy/Δx]
d	mass shift distance	[m]
r	pendulum reading/deflection	[m]
L	pendulum length	[m]
HZ	heeling arm	[m]
HZ_0	initial heeling arm	[m]
HZ_i	heeling arm for individual weight shifts	[m]
GZ	righting arm	[m]
BM	metacentre-buoyancy radius	[m]
GM	height of metacentre from centre of gravity	[m]
KN	righting arm about origin	[m]
KN_0	initial righting arm about origin	[m]
KN_i	righting arm about origin for individual weight shifts	[m]
KM	height of metacentre from keel	[m]
G_0G_i	system weight-shift distance for individual weight	[m]
LCG	longitudinal centre of gravity	[m]
TCG	transverse centre of gravity	[m]
VCG/KG	vertical centre of gravity	[m]
TCB	transverse centre of buoyancy	[m]
LCB	longitudinal centre of buoyancy	[m]

1. Introduction

The inclining experiment is the primary method available for determining the vertical centre of gravity, VCG, of the lightship of a vessel upon completion and to keep track of any changes in VCG through the vessel's life. There are alternatives such as the roll period test, but no other method is as feasible and as broadly accepted as the classical inclining experiment in use today. It is, however, a well-known fact that the current method, the so called *Classical* method, in which we calculate the vessel VCG following inclining experiments has its limitations on performance in terms of applied heel angle magnitude and accuracy for certain hull-forms. This is due to the assumption made of unchanged metacentre position when the vessel is heeled. The method validity has therefore been a topic of considerable discussion and debate through the years. The *Classical* method seems, however, to have prevailed despite the universal knowledge of limiting assumptions as will be discussed in this paper. Recently, alternative methods in calculating the VCG, following inclining experiments, have been proposed and are stated to have improved accuracy and flexibility on vessel-type and inclining heel angles. The so-called *Generalised* method was initially proposed by R.J. Dunworth (2013) and further expanded in Dunworth (2014, 2015) and Smith, Dunworth & Helmore (2016). Another method, named the *Graphical* method was proposed by Kanifolskyi & Konotopets (2016). Finally, a third method named the *Polar* method has been developed by the first author and will be presented in this paper.

2. Approach

The study presented in this paper, aims to test the various methods available for calculating a vessel's centre of gravity following an inclining experiment on a range of vessels. The tests comprise firstly purely technical inclining experiments performed in the stability software NAPA to establish error potential for each method. This is performed for three different heel angles, i.e., 2, 4, and 10 degrees. This approach excludes any errors resulting from external disturbances or incorrect measurements. This will ensure that the ensuing errors are purely a result from the calculation

method used. The technical experiments are expected to shed some light on each method as well as on which method produces the most accurate results. This derives from the fact that the calculated results for the VCG can be checked against VCG values specifically given the loading condition created in the stability software, and produce error potentials for each method using the percentage difference. Secondly, the methods have been applied to real physical inclining experiment readings from the same vessels used in the technical experiments. Using the established error potential resulting from the technical experiments, a corrected VCG is derived from the physical VCG values. The new corrected VCG values have been evaluated against the loading conditions for each vessel to see if the stability margins have been exceeded as well as obtain an indication on whether the Classical method has compromised safety in the operation of the vessels in question. Finally, recommendations and suggestions for each of the methods will be provided.

3. Background

According to SOLAS Reg. II-1/5 (IMO, 2009), every passenger ship, regardless of size, and every cargo ship above 24 meters in length, shall be inclined upon its completion or following any design alterations affecting stability. High-speed and light-craft have similar requirements as found in the HSC Code Reg. II/2.7 (IMO, 2000), and in Torremolinos Reg. III/9 (IMO, 1977 as amended), for fishing vessels. Even smaller recreational craft above 6 meters in length have equivalent requirements in ISO standard 12217-2 (ISO, 2013). Passenger vessels are according to SOLAS further required to be inclined every 5 years if lightweight surveys identify a weight change above a certain threshold limit. Lightweight change through a vessel's life is very common, especially for passenger vessels as they often are refurbished and converted through their operating-life. This is clearly highlighted in Table 1.

Table 1: Weight change for typical large passenger vessel

Year	Δ [tonnes]	dΔ [tonnes]	VCG [m]	dVCG [mm]
2006	30112.51	803.29	18.46	-115.00
2011	29802.12	-310.39	18.63	170.00
2016	29453.45	-348.67	18.8	172.00

Before a vessel's stability in any condition of loading can be assessed, its initial lightweight condition needs to be known. It is from this condition that all other loading conditions are created, applying loads in terms of cargo, crew, consumables and other equipment, and checked against given stability criteria. It can therefore be considered as the vessel's main stability reference and measure of loading capacity. Any errors in determining the lightweight particulars will therefore be a consequential error on all other loading conditions that are to be assessed against relevant intact and damage stability criteria. An incorrect lightship VCG could in the worst case overestimate the vessel stability margins and compromise vessel safety. On the other hand, if the VCG is overestimated, the vessel loading capacity will subsequently be reduced. This shows the importance in using the most accurate method in determining the VCG in the lightweight condition.

4. Classical method assumption

The Classical method's validity is based on the assumption that the position of the metacentre is unchanged when the vessel is heeled. The position of the metacentre can be represented by the metacentre-radius (BM) given by the well-known relationship (1) between the transverse second-moment of the waterplane area (I_{XX}) and the vessel's displaced volume (∇):

$$BM = \frac{I_{XX}}{\nabla} \tag{1}$$

As the vessel's displaced volume is constant during the incline, the change in the metacentre position is proportional to the change in the second moment of the waterplane area, and consequently the waterplane area itself. For small heel angles (0-4 degrees), the change in the waterplane area can be disregarded for most conventional vessels, especially for wall-sided vessels

where equal wedges of buoyancy volume are immersed and submerged when heeled. This has given rise to the so-called wall-sided assumption.

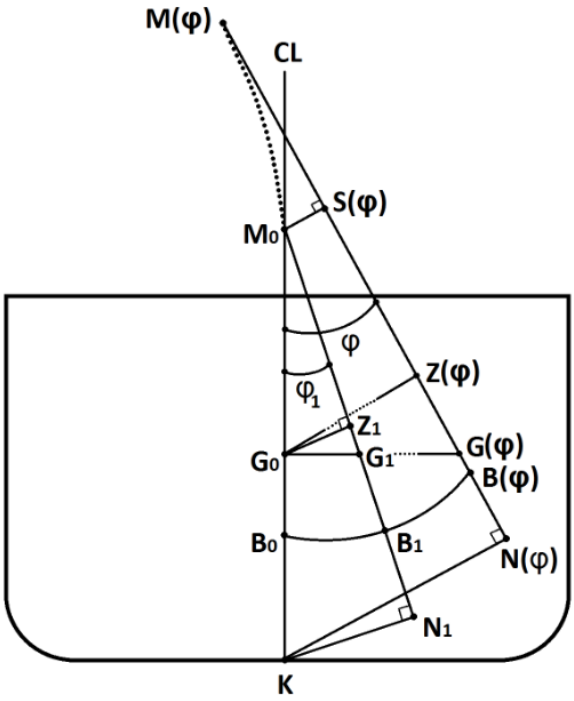

Fig. 1: Traditional stability parameter representation

The position and movement of the metacentre for small and large heel angles have been illustrated in Figure 1 by M_0 and $M(\varphi)$ respectively. The actual movement of the metacentre can be seen in Appendix A and C for all test vessels. Assuming small heel angle, φ_0, the trigonometric relationships from Figure 1 in combination with the weight-movement relationship in (4), leads to the well-known formulation of the *Classical* method as deduced in the following. The $\tan(\varphi)$ can be represented directly by the pendulum relationship in (6).

$$\tan(\varphi) = \frac{G_0G_1}{G_0M_0} \tag{2}$$

$$G_0M_0 = \frac{G_0G_1}{\tan(\varphi)} \tag{3}$$

$$G_0G_1 = \frac{w \cdot d}{\Delta} \tag{4}$$

$$GM = G_0M_0 = \frac{w \cdot d}{\Delta \cdot \tan(\varphi)} \tag{5}$$

$$\tan(\varphi) = \frac{r}{L} \tag{6}$$

The position of the metacentre is, however, not constant for wall sided ships and even a completely box-shaped vessel will show change in the position due to change in waterplane area as is illustrated in Figure 2 for various heel angles (0-360°).

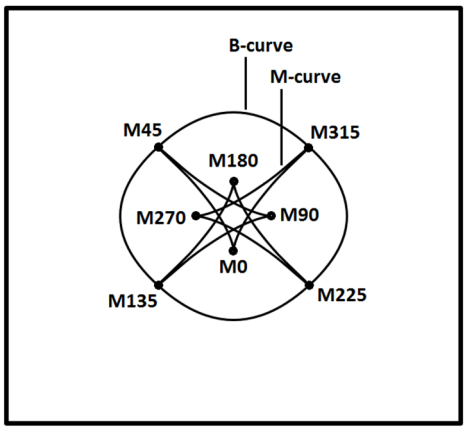

Fig. 2: Box-shaped vessel with movement of B and M

If the metacentre is to be unchanged when the vessel is heeled, the vessel form needs to be assumed completely circular as is illustrated in Figure 3.

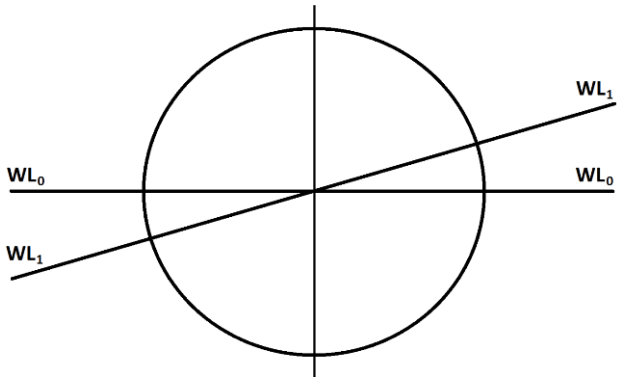

Fig. 3: Circular hull form with constant waterplane area

Considering the above, ships that are prone to inaccuracies using the *Classical* method must comprise ships where the waterplane area changes significantly when heeled, such as ships with knuckles, large flare angles, sharp chine lines and other unconventional hull forms. It is often smaller vessels that have such designs, which are particularly affected by wrongful assumptions in the

Classical method. Furthermore, it is the smaller vessels, which are more affected by errors caused by disturbances from external influences such as wind, waves, current, etc.

5. The inclining experiment

This section will briefly explain the main tasks of the inclining experiment. More detailed description and guidelines for how to perform inclining experiments can be found in IMO 2008 IS Code Part B Annex I (IMO, 2008) and IACS Rec.31 (IACS, 1990). Classification societies also have their own guidelines, e.g. DNVGL-CG-0157 Annex I (DNV GL, 2016). The inclining experiment comprises three main tasks, namely the *inclination*, a *draught survey* and a *weight survey*, each explained briefly in the following:

5.1 Inclination

During the inclining experiment, the ship is deliberately heeled by transverse movement of known weights, w, a known distance, d, during several shifts. Normally, 8 shifts are conducted for satisfactory results and in the traditional sequence as is illustrated in Figure 4.

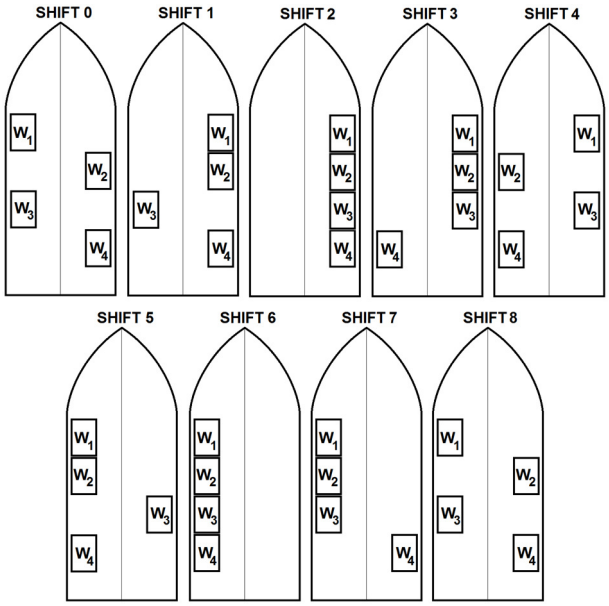

Fig. 4: Traditional weight shift sequence

For each shift, the change in equilibrium angle from initial position is found by measuring the deflection obtained in pendula placed on board the vessel. Other devices of finding the deflection can be used such as U-tubes. Normally 2 or more devices are used during an experiment for satisfactory results. The weight shifts are normally conducted using mass weights but it could also be conducted by transfer of ballast-water in tanks. If ballast-water is used, special consideration should be taken, as explained in more detail in IMO 2008 IS Code Part B Annex I Ch. 2.3.4 (IMO, 2008). From the pendula deflection readings, the heeling angle for each shift is obtained and together with the known moment for each shift, given by $w \cdot d$, sufficient information is obtained for applying all three calculation methods. The methods are explained further in Section 7.

5.2 Draught survey

The draught survey is conducted to determine the vessel's displacement during the experiment. Draught readings are taken to determine the so-called *as inclined* floating position, which is the actual loading condition of the vessel when the inclining experiment is taking place. This includes all weights in excess of the lightweight, comprising liquid in tanks, on-board personnel, equipment and inclining weights. Relevant hydrostatic data can then be found based on the draught readings using computer software or tabulated values.

5.3 Weight survey

The weight survey is performed in order to make inventory of the weights on-board during the incline. This includes missing weights that are to be taken on board following the experiment, temporary weights that are to be removed following the experiment and weights that are to be moved to a new location following the experiment. Liquids in tanks should be minimal but if needed tanks should be pressed full for reduction in Free Surface Moment (FSM) correction. Any FSM correction needs to be noted and accounted for in the calculation of the VCG. The inventory of weights is then used to calculate backwards from the *as inclined* condition obtained in the *draught survey*, to find the lightweight condition.

6. Uncertainty and errors

It is well-known that inclining experiments are subject to a range of sources of uncertainties and errors originating from external influences such as wind, waves, current and human measurement errors. This paper focuses only on the error originating from the choice of calculation method. Other sources of uncertainty and errors have been reviewed and discussed in many publications, such as Shakshober & Montgomery (1967) and Woodward et al. (2016). It is, however, important to mention that the methods themselves can show different degree of sensitivity to the various sources of uncertainty and errors. Such sensitivity will not be identified using a *technical* approach as is used in this study, hence, such sensitivity analysis has not been included at this point. For more detailed information on the range of uncertainties related to the inclining experiment, the above mentioned publications are recommended but to highlight the most common sources of uncertainty, Figure 5 below has been borrowed from Woodward et al. (2016).

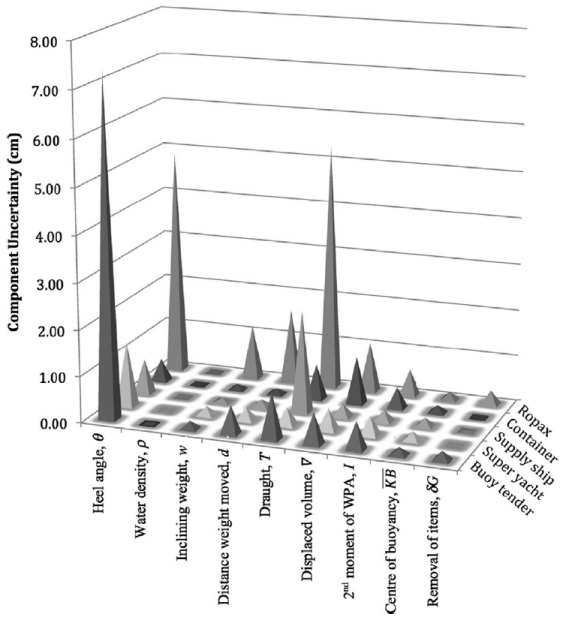

Fig. 5: Component uncertainty contribution for various inclining experiment parameters. Reprinted by permission from Woodward (2016, fig. 2)

The figure show the various sources of component uncertainty contribution in the vertical centre of gravity for various inclining experiment parameters for five case study vessels. The figure

clearly indicates that the highest contribution is originating from the heel angle and draught in terms of uncertainties related to pendula and draught marks.

7. Inclining experiment methods

This chapter will explain each of the four calculation methods in terms of derivation, assumptions and application. The *Classical* method is explained first, followed by the newly proposed methods.

7.1 The Classical method

The *Classical* method uses relation (5) as derived in Section 4 as the basis for calculating VCG. For each weight-shift the obtained moment $w \cdot d$ from the weight movement is plotted against $\tan(\varphi)$ obtained from the pendula deflection relationship (6), as is shown in Figure 6.

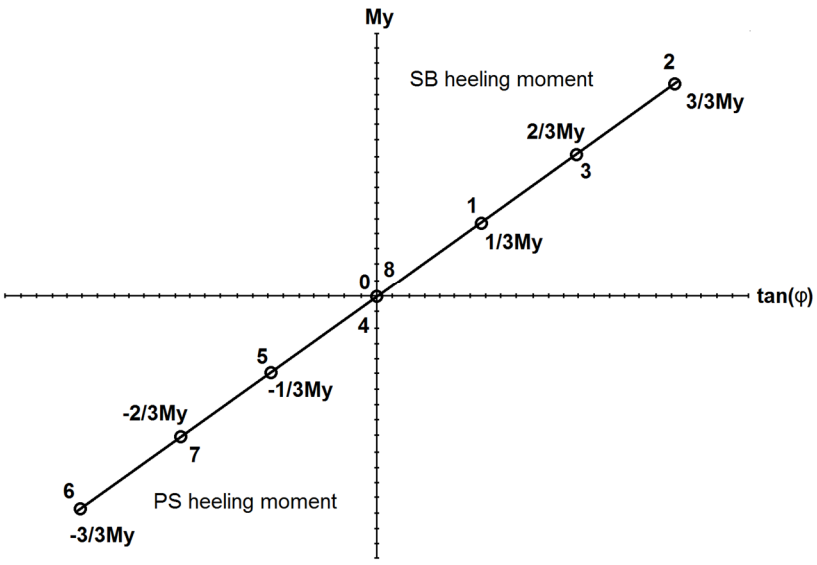

Fig. 6: Plot of moment against $\tan(\varphi)$, including regression slope

The linear regression can then be calculated using a least square fit and the GM can be calculated using the following:

$$GM = \frac{1}{\Delta \cdot R_{slope}} \tag{7}$$

Alternatively, each value of $w \cdot d/\Delta$ can be plotted against $\tan(\varphi)$ and the value of GM can directly be calculated as the regression slope using a least square fit. The value of VCG can finally be calculated using (8). The free surface correction is found during the *weight survey* and the KM value is found from hydrostatic data following the *draught survey*. As free surface will induce a higher heel angle than the weight shift alone due to transverse and vertical shift of the liquid's centre of gravity, it is important to note that the FSM correction shall be deducted from the VCG directly rather than added to the heeling arm as is normal in traditional stability calculations when considering FSM correction on the GZ-curve.

$$VCG = KM - GM - FSM \tag{8}$$

The remaining transverse and longitudinal centre of gravities are found using formulae (9) and (10).

$$TCG = TCB_{\varphi=0} + \tan(\varphi) \cdot GM \tag{9}$$

$$LCG = LCB - \frac{Trim \cdot MCT \cdot 100}{\Delta} \tag{10}$$

7.2 The Generalised method

Details behind the *Generalised* method can be found in Dunworth (2013, 2014, 2015) and Smith, Dunworth & Helmore (2016). The method is based on the fact that when the vessel reaches equilibrium for each weight shift the vessel's righting moment and heeling moment must be equal and according to Newton's 2nd law it follows:

$$\sum M_Y = 0 \tag{11}$$

$$H_{mom} = R_{mom} \tag{12}$$

$$\Delta \cdot HZ = B_M \cdot GZ \tag{13}$$

As illustrated in Figure 7, the displacement- and buoyancy forces are equal, i.e. $\Delta = B_M$, subsequently the heeling- and righting arms are equal in the equilibrium position, i.e.:

$$HZ = GZ \tag{14}$$

Using the trigonometric relationships as illustrated in Figure 7, the following relationship can be derived:

$$HZ = KN - KG \cdot \sin(\varphi) - TCG \cdot \cos(\varphi) \tag{15}$$

Rearranging this equation, the final equation is obtained for finding the vertical centre of gravity as follows (please note that Dunworth uses the designation KG for the vertical centre of gravity).

$$KG \cdot \sin(\varphi) = KN - HZ - TCG \cdot \cos(\varphi) \tag{16}$$

$$HZ = \frac{w \cdot d \cdot \cos(\varphi)}{\Delta} \tag{17}$$

$$KG \cdot \sin(\varphi) = KN - \frac{w \cdot d \cdot \cos(\varphi)}{\Delta} - TCG \cdot \cos(\varphi) \tag{18}$$

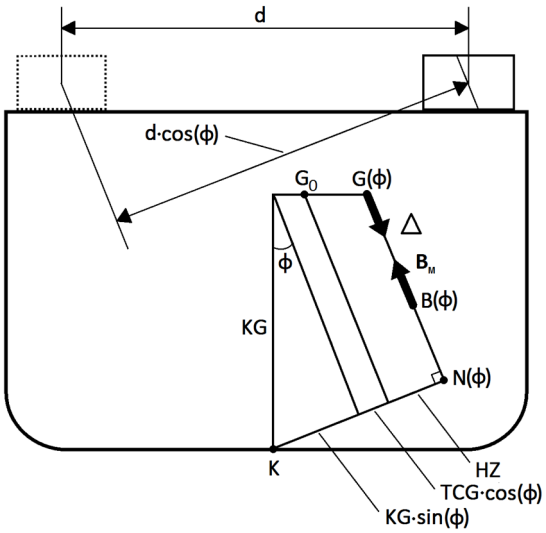

Fig. 7: Main parameters during vessel incline. Adapted from Dunworth (2014)

To this end, actual KN values are needed from a stability software model, corresponding to equilibrium position for each weight shift. The heeling angle is determined from the pendulum deflection relationship (6) similar to the *Classical* method. For each shift $KG \cdot \sin(\varphi)$ is calculated using equation (18) and plotted against $\sin(\varphi)$. The final value of KG can be directly calculated as the regression slope using a least square fit similar to the *Classical* method. From the above, it is apparent that this method does not make any reference to the metacentre in the calculations and

should therefore not be influenced by any change in the waterplane area during the weight shifts, as is the case for the *Classical* method. Dunworth (2013) further suggests an alternative method for calculating the TCG offset in the initial position, i.e., when inclining weights are in *neutral* position. In this respect, the following can be derived:

$$TCG = KN_0 - HZ_0 \tag{19}$$

Dunworth's derivation is as follows: for a symmetrical ship where $KN_0 = 0$, the TCG equals the heeling lever HZ_0 in the upright position. HZ_0 can be determined by plotting the heeling lever HZ against heel angle φ using (17). HZ_0 then equals the intercept with the y-axis when heel angle is $\varphi = 0$. Dunworth proposes to find the intercept by fitting a third-order polynomial to the points as is illustrated in Figure 8. The remaining longitudinal centre of gravity are found using (10) similar to the *Classical* method.

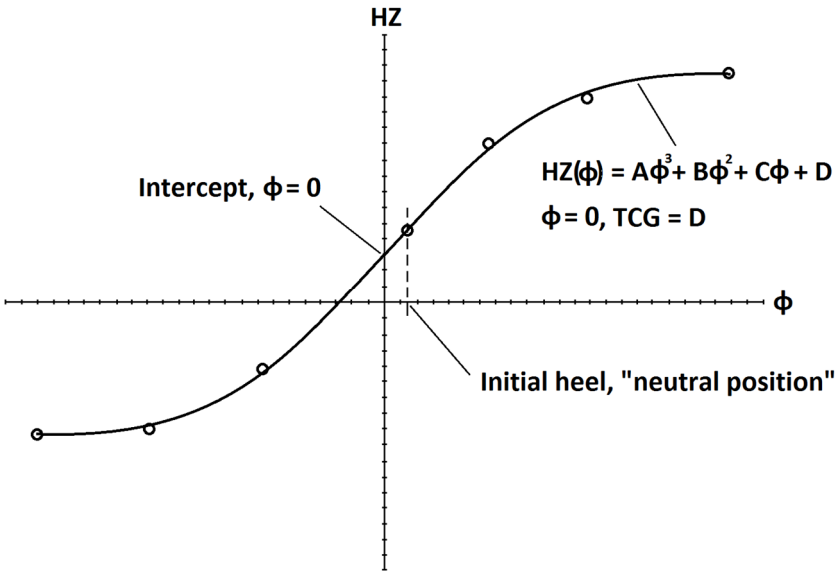

Fig. 8: Third-order polynomial fit to HZ_i as a function of φ

7.3 The Graphical method

The *Graphical* method, as indicated by its name, is performed by graphical representation of the relationships depicted in Figure 9. Similarly to the *Generalised* method, KG is used as designation for the vertical centre of gravity and actual KN values are needed from a stability software model, for

the actual floating position corresponding to each weight shift. An alternative method when a computer software model is not available, involving construction of Tchebysheff's sections is described in Kanifolskyi & Konotopets (2016) but for testing of the method in this paper, real KN values from computer software have been used. Using the heel angle obtained for each shift using (6), it is as a first step possible to graphically draw KN from the keel point, K, outward with the correct heel angle φ. As a second step, the perpendicular to KN can be drawn and as a third step HZ is calculated using equation (17). In the fourth step, the calculated HZ arm is placed in its correct position, i.e. where it's distance from the KN-perpendicular equals the HZ distance and intercepts the centreline. In the fifth and final step, the VCG, or KG distance, can be measured. All steps are depicted in Figure 9 below.

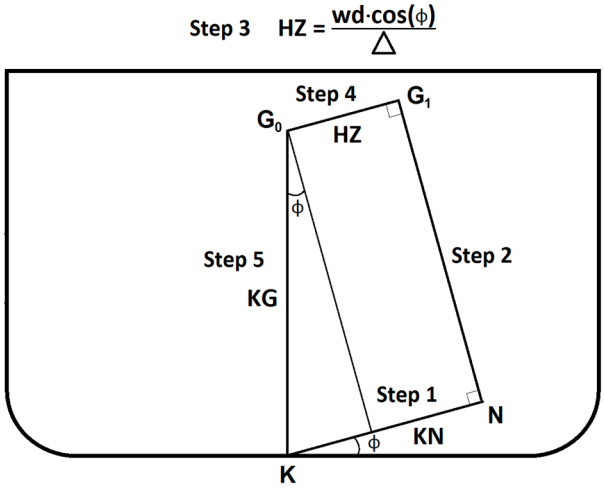

Fig. 9: Graphical representation of parameters during vessel incline

According to Kanifolskyi & Konotopets (2016), the described steps should be performed graphically in a Cad-software for best accuracy. The final KG is then calculated as the average KG from all steps performed in the experiment using (20).

$$KG = \frac{\sum_{i=1}^{n} KG_i}{n} \tag{20}$$

Instead of drawing the distances graphically as is proposed, it is suggested that it should be possible to find KG for each weight shift from a trigonometric perspective using Figure 9. When knowing KN and the heel angle φ, KG can be found by using the following:

$$KG = \frac{KN - HZ}{\sin(\varphi)} \tag{21}$$

$$KG \cdot \sin(\varphi) = KN - HZ \tag{22}$$

$$KG \cdot \sin(\varphi) = KN - \frac{w \cdot d \cdot \cos(\varphi)}{\Delta} \tag{23}$$

From the above, and by comparing equations (18) and (23), it is clear that the *Graphical* method is a graphical application of the *Generalised* method, but without considering the TCG offset as is included in (18). This seems to be the reason for the *Graphical* method being limited to a maximum initial heel of 0.5 degrees. Any higher initial heel angles will cause proportionally higher errors from the real KG value. It is further believed that if the regression slope is used rather than using the averaged, the results would be more accurate despite not considering the TCG offset. As for the *Classical* method, the remaining centre of gravities can be found using (9) and (10).

7.4 The Polar method

The Polar method is a new suggestion developed during this study. The method considers the line parallel to the BM radius, shifted a distance HZ, and represented in polar coordinates, hence the name. The method takes advantage of the fact that both VCG and TCG need to be located on this line in the initial condition and be kept constant in this position for each individual weight shift. To be more specific, the initial VCG_0 and TCG_0 are kept constant on this line, while the overall system TCG is shifted a distance G_0G_i for each shift i. The line is illustrated in Figure 10.

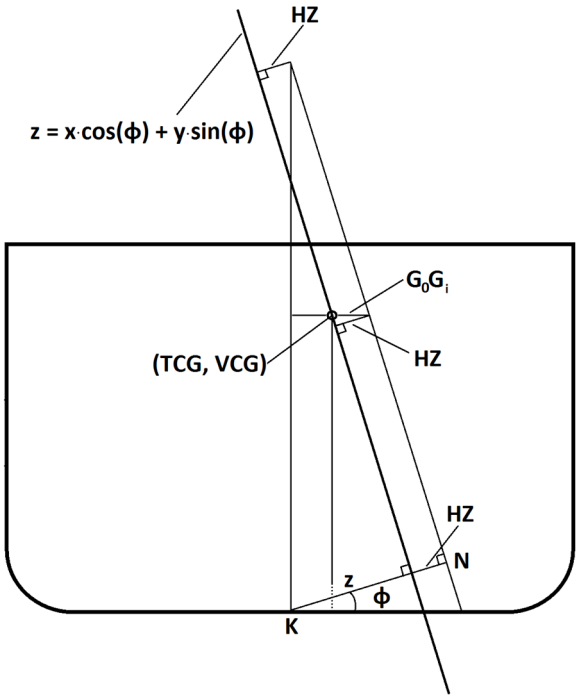

Fig. 10: Parameters of the Polar method

The equation for the line is given by (24), and knowing that the x-coordinate is equal to the TCG, and the y-coordinate is equal to the VCG, we obtain equation (25).

$$z = x \cdot \cos(\varphi) + y \cdot \sin(\varphi) \tag{24}$$

$$z = TCG \cdot \cos(\varphi) + VCG \cdot \sin(\varphi) \tag{25}$$

From Figure 10, it is also apparent that z can be represented by (26), resulting in (27):

$$z = KN - HZ \tag{26}$$

$$KN - HZ = TCG \cdot \cos(\varphi) + VCG \cdot \sin(\varphi) \tag{27}$$

Considering the above and taking advantage of the fact that VCG_i and TCG_i for each shift i, must be equal to VCG_0 and TCG_0 in the initial, or *neutral* position, there are now available two equations, (28) and (29), to derive the two unknown parameters.

$$TCG_i = TCG_0 \tag{28}$$

$$VCG_i = VCG_0 \tag{29}$$

Using (27) and following some deduction, (28) results in a solution for VCG given by (30) and (29) in a solution for TCG given by (31) in their most general form.

$$VCG = \frac{(KN_i - HZ_i)\cdot\cos(\varphi_0) - (KN_0 - HZ_0)\cdot\cos(\varphi_i)}{\cos(\varphi_0)\cdot\sin(\varphi_i) - \sin(\varphi_0)\cdot\cos(\varphi_i)} \tag{30}$$

$$TCG = \frac{(KN_i - HZ_i)\cdot\sin(\varphi_0) - (KN_0 - HZ_0)\cdot\sin(\varphi_i)}{\sin(\varphi_0)\cdot\cos(\varphi_i) - cos(\varphi_0)\cdot sin(\varphi_i)} \tag{31}$$

As the heeling arm in the initial position is zero, since $d = 0$, the final representation for VCG and TCG results in the following:

$$VCG = \frac{(KN_i - HZ_i)\cdot\cos(\varphi_0) - (KN_0)\cdot\cos(\varphi_i)}{\cos(\varphi_0)\cdot\sin(\varphi_i) - \sin(\varphi_0)\cdot\cos(\varphi_i)} \tag{32}$$

$$TCG = \frac{(KN_i - HZ_i)\cdot\sin(\varphi_0) - (KN_0)\cdot\sin(\varphi_i)}{\sin(\varphi_0)\cdot\cos(\varphi_i) - cos(\varphi_0)\cdot sin(\varphi_i)} \tag{33}$$

From equations (30) and (31) various assumptions may be accounted for. If the vessel is upright in the initial position, i.e. initial heel angle $\varphi_0 = 0$, the equations are reduced to the following:

$$VCG = \frac{(KN_i - HZ_i) - (KN_0 - HZ_0)\cdot\cos(\varphi_i)}{\sin(\varphi_i)} \tag{34}$$

$$TCG = KN_0 - HZ_0 \tag{35}$$

Further, knowing that the initial heeling arm is zero and if the vessel is both upright and completely symmetrical, i.e. the initial $KN_0 = 0$, they reduce to:

$$VCG = \frac{KN_i - HZ_i}{\sin(\varphi_i)} \tag{36}$$

$$TCG = 0 \tag{37}$$

Equation (35) substituted in (34) reduces to (18). This indicates that the *Generalised* method is only valid for upright vessels in the initial condition, despite accounting for the TCG offset, while the *Polar* method is more general as it accounts for any initial heel angle φ_0. It is further shown that (36) has been reduced to (21), indicating that the *Graphical* method is only valid for symmetrical vessels, and confirming its limitation of only being valid for vessels being upright in the initial condition.

Finally, (37) can be regarded as proof of the equations and assumptions used by deriving the *Polar* method, as it confirms that a symmetrical vessel with no heel will have a TCG of zero. When applying the *Polar* method, equations (32) and (33) shall be used and similar to the *Classical-*, and the *Generalised* methods, the slope of the regression line for all shifts is used to calculate the VCG and TCG respectively, i.e. numerator plotted against the denominator of the equations. Similarly to the *Generalised-* and *Graphical* methods, actual KN values are needed from a stability software model, HZ values are calculated using (16), and the remaining longitudinal centre of gravity can be found using (10).

8. Technical inclining experiment

The *technical* inclining experiment has been performed in the stability software *NAPA* for 9 different vessel types, which are presented in Section 10. Each of the vessels have been given lightweight and inclining weights in the stability software, such that total displacement and floating position in the *as inclined* condition is equal to the *physical as inclined* conditions from the real inclining experiments described in Section 9. In the *technical* incline the vessels were free to both heel and trim, following each weight shift. The *technical* inclining experiment was performed using both small and large heel angles. Smaller heel angles of 2 and 4 degrees were chosen, as 4 degrees is the largest heel angle allowed in accordance with IMO 2008 IS Code Part B Ch. 8.2.2.8 (IMO, 2008). The large heel angle was chosen to be 10 degrees. Such extreme heel angles will not be practical in an actual inclining experiment, but have been included in this study for the purpose of highlighting the validity of the methods for extreme heel angles values. The inclining weights and subsequent displacement were kept the same for both the small and large heel angle inclines. Differences in heel angles, imposed by a difference in moment, have been obtained by applying a larger moved weight distance. A macro was produced in *NAPA*, enabling the weights to be shifted and relevant hydrostatic values extracted for each weight shift. These were applied in the various methods for calculation of the *technical* VCG and TCG values. The results for each of the various methods were

checked against the lightweight particulars specifically given to the *as inclined* condition for each vessel in the stability software *NAPA* and an error potential could be developed in [mm] and in [%] difference from the calculated of VCG and TCG values. The error potential can be seen as a measure of accuracy for each of the methods. Calculating a smaller VCG than the actual value indicates an underestimation while a higher VCG indicates an overestimation.

9. Physical inclining experiment

Real inclining experiment readings were obtained for all the vessels from actual inclining experiments. These reflect their current lightweight condition applied in their stability booklets as approved by the administration. Inclining experiment readings have been applied to all four calculation methods and *physical* VCG and TCG values have been obtained. Knowing the potential error from the *technical* VCG and TCG, the *physical* values were corrected accordingly to account for the obtained error potential, i.e. if the error potential indicated underestimation or overestimation, the actual value has been increased or decreased accordingly. Each of the corrected VCG values have been used to check if the stability margins for the worst loading conditions have been exceeded and safety compromised. Similarly, an overestimated stability margin would affect the vessel loading capacity, and subsequent earning potential.

10. Test vessels

Main particulars for the vessels chosen for testing of the calculation methods are presented in Table 2. The test vessels comprise 9 vessels of various type, size and hull form to account for the ship specific problematic design features, such as knuckles, large flare angles, sharp chine lines and other unconventional hull attributes. More conventional wall-sided hull forms have been included as well for comparison. Lines plans for all vessels are presented in Appendix D.

Table 2: Test vessel particulars

Vessel type	L_{BP}[m]	B [m]	D [m]	C_B[-]
Fishing Vessel	40.20	12.00	7.50	0.73
Yacht	36.60	7.70	4.20	0.54
RoPax	195.30	25.80	14.80	0.79
Bulk Carrier	223.50	32.30	20.20	0.92
Passenger Vessel	320.20	41.40	11.60	0.74
Naval I	54.10	10.60	5.00	0.65
Naval II	71.00	12.00	6.20	0.58
Container Vessel	320.00	48.20	27.20	0.76
Supply Vessel	76.80	19.50	7.75	0.69

11. Results

In this section, only a pictorial summary of the results is presented. Complete detailed tabulated results are presented in Appendix E. The results for the calculated VCG values from the *technical* inclining experiments are presented first. In order to compare the methods against each other, the result is represented by the absolute-value of the percentage-error potentials, irrespectively of over-, or underestimation. No detailed results for the TCG calculations have been included in this section. From Appendix E, it is shown that all the methods are producing viable results for the TCG values, with maximum error of 1% for all vessel types and heel angles. Only a short summary of the TCG results has therefore been included. Finally, the VCG results for the real *physical* inclining experiment readings are presented, including new corrected VCG values considering the error potential and their influence on the stability margins. It should be noted that only the vessels where the VCG has been underestimated have been included for this purpose. Overestimation is only affecting loading capacity and is considered of secondary importance in this study.

11.1 Technical inclining experiment results

As mentioned in the foregoing, the various methods have been applied for 2, 4 and 10 degrees of maximum inclining heel angles, using for each of these initial heel angles of 0, 0.5 and 1 degrees.

This results in a total of $3 \cdot 3 = 9$ different cases that have been applied using each of the calculation methods. In the following, each of these combinations will be presented in graphs covering all the methods together for comparison. It is important, however, to note that the errors obtained when applying the *Graphical* method as it is intended, are extensive compared to the other methods when calculated for any of the initial heel angles other than zero. Because of this, the *Graphical* method, when calculated with initial heel $\varphi_0 > 0$, is presented separately for better presentation and comparison of the other methods. The absolute values of the percentage errors averaged over all vessel types using the *Graphical* method are shown in Figure 11 to illustrate the large errors. Detailed results can be found in Appendix E.

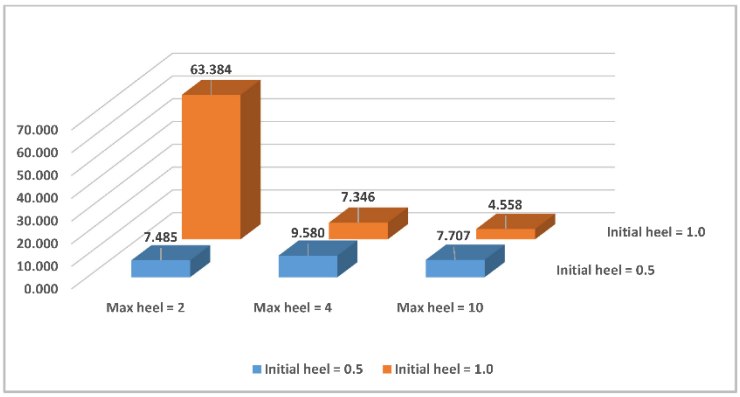

Fig. 11: Percentage error for VCG averaged over all vessels using the Graphical method with initial heel angles

There seems to be two reasons for the extensive errors when using initial heel angles $\varphi_0 > 0$ when applying the *Graphical* method. The first being the fact that the distance HZ between the KN perpendicular and the centreline, does not account for the TCG offset (step 4 explained in Section 7). It will therefore overestimate the VCG distance for weight shifts towards the side with the initial heel by an amount of $TCG/\tan(\varphi)$ and likewise underestimate the same amount for opposite weight shifts. One would expect this to be evened out by using the averaged value but this is evidently not the case. The heel angle to each side will be different due to the initial heel and by assuming a constant moment to each side using the same weights and shift distance, the underestimation towards the opposite side of the initial heel angle will be larger than the

overestimation, resulting in an averaged overall underestimation. This is assuming an even number of negative and positive heel angles from all the shifts. If a large initial heel is used and the intermediate weight shifts are not large enough to make the vessel heel to the opposite side, this may result in an uneven number. This is confirmed by the detailed results in Appendix E as it leads to large overestimation for all vessels for cases with initial heel angles greater than zero. This is due to the choice of initial heel angle to the positive starboard side, resulting in a higher number of positive heels, hence an overall overestimation. The second reason for the errors is that when applying initial heels, some of the intermediate weight shifts may produce heel angles close to zero, which results in KN values close to zero. This makes it very difficult to solve the problem graphically. In these cases, the mathematical representation of the *Graphical* method, represented by (21), also produces unreliable results due to $\sin(\varphi) \to 0$, for $\varphi \to 0$, resulting in division by zero. The only way of accounting for this, is to apply the linear regression used for the other methods. When applying the *Graphical* method in this study, such cases have been omitted when averaging the VCG values. For assessing the mathematical representation of the *Graphical* method using linear regression, results have been included together with the other methods for comparison, as it produces smaller errors than the graphical representation for cases with initial heel angles greater than zero. The application of the *Graphical* method is further discussed in the Conclusions section. Firstly, for presenting the results, the three cases with initial heel of 0 degrees are presented, i.e. vessel upright. For the upright cases, as mentioned above, both the graphical and mathematical representation of the *Graphical* method have been included, indicated by *Graphical_G* and *Graphical_M*, respectively. Only the *Classical* method has been included with data labels for a tidier presentation, as the other methods all have obtained errors below 0.1% as seen in Appendix E. In Figure 12, the inclining angle of 2 degrees is presented. From the figure, it is clear that all methods produce accurate results, with the highest error below 0.5%, obtained by the *Classical* method for the Naval II vessel. In Figure 13, maximum heel angle of 4 degrees is presented. The results still show good accuracy for all methods, but the *Classical* method's error is now increased to 1.5% for the Naval II vessel. In Figure 14,

maximum heel angle of 10 degrees is presented. As expected, the results show much lower accuracy for the *Classical* method, with a maximum error above 6% for the Naval II vessel. All the remaining methods still show high accuracy, with only an error of below 0.02%. To summarise the upright cases, Figure 15 presents the error potential averaged over all vessel types for all methods for the various inclining heel angles. It is clearly shown that the *Classical* method is highly dependent on the inclining heel angles compared to the other methods.

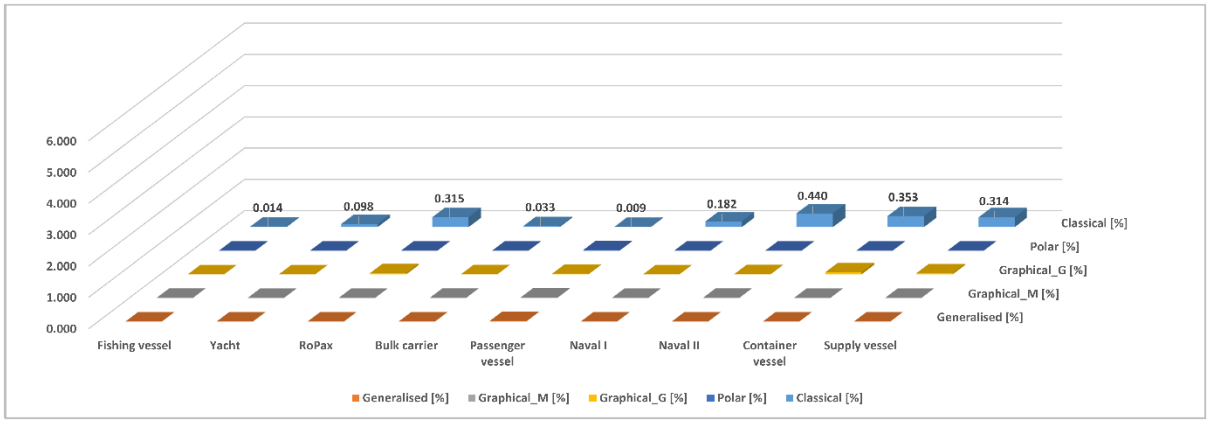

Fig. 12: Percentage error for VCG, 2 degrees maximum heel angle and 0 degrees initial heel angle

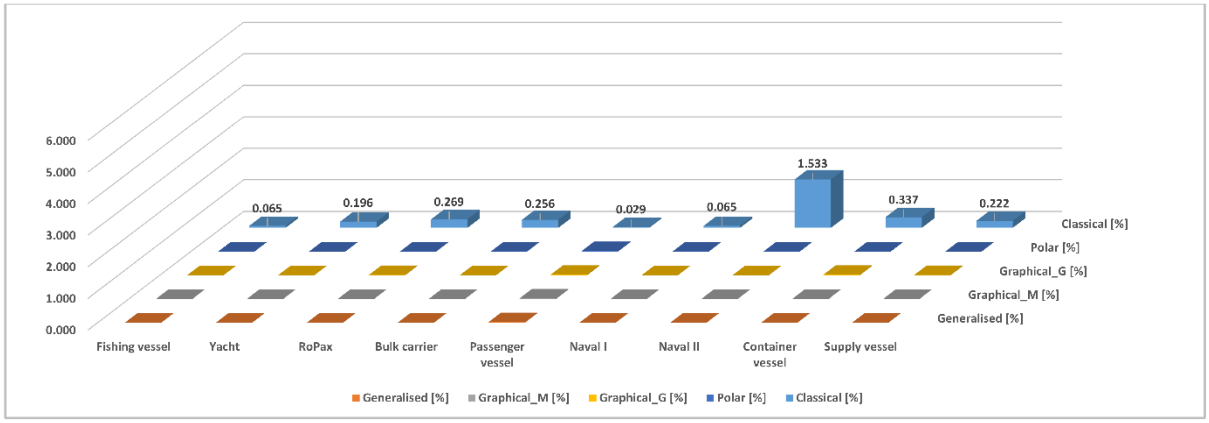

Fig. 13: Percentage error for VCG, 4 degrees maximum heel angle and 0 degrees initial heel angle

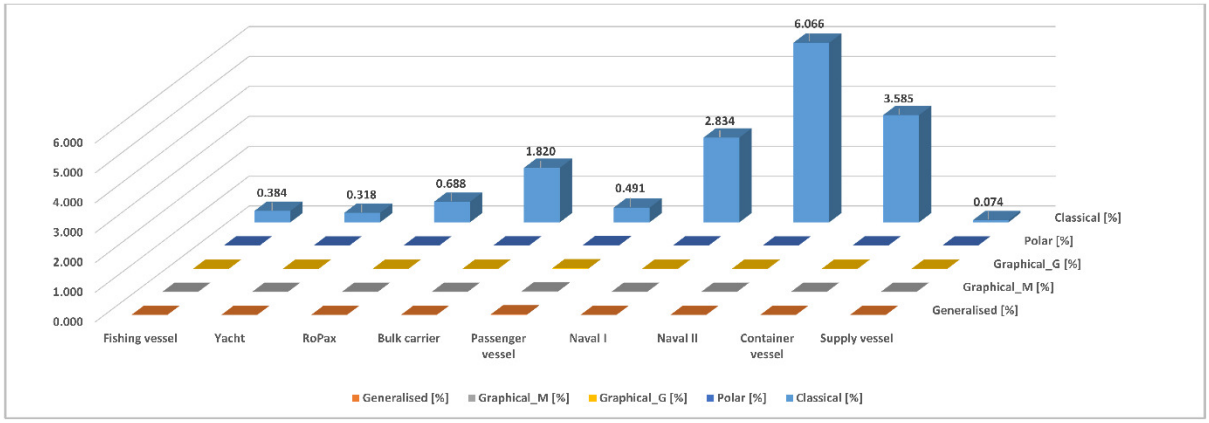

Fig. 14: Percentage error for VCG, 10 degrees maximum heel angle and 0 degrees initial heel angle

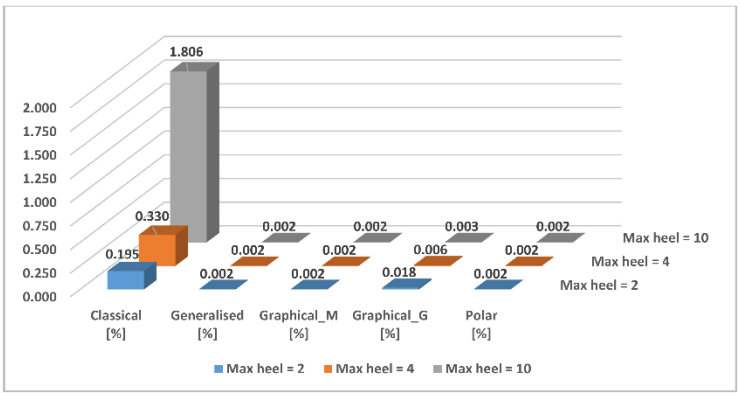

Fig. 15: Error potential averaged over vessel types, various heel angles and methods, 0 degrees initial heel

Secondly, the three cases with initial heel of 0.5 degrees are presented. Here, only the mathematical representation of the *Graphical* method has been included, due to the high errors of the graphical representation. The subscript $\_M$ is now removed, and the mathematical representation is designated *Graphical* in the following. As before, the maximum inclining angle of 2 degrees is presented firstly in Figure 16, followed by 4 and 10 degrees in Figure 17 and 18. A similar trend to that of the upright cases is seen. As before, the *Classical* method is seen to be highly dependent on the heel angle magnitude, as the error increases significantly for larger heel angles, increasing from 0.5-1% for the smaller heel angles to over 5.5% for the larger heel angle. All the remaining methods still show high accuracy, with only an error of below 0.02%, similar to the upright cases. Again, to summarise, Figure 19 presents the error potential averaged over all vessel types for all methods for the various inclining heels. It is again clearly shown that the *Classical* method is

highly dependent on the inclining heel angles compared to the other methods. The errors are slightly lower for some of the cases with initial heel of 0.5 degrees, compared with the upright cases. The reason is due to the movement direction of the metacentre and not only the magnitude of the movement as will be discussed later in further detail.

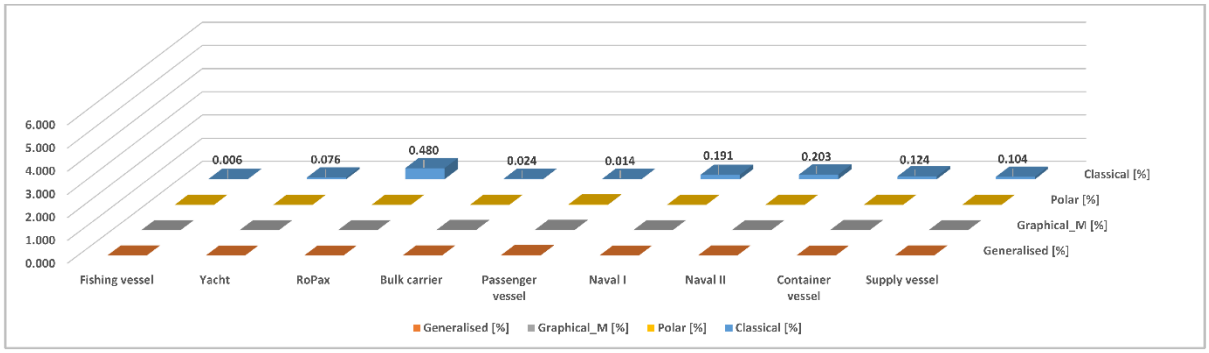

Fig. 16: Percentage error for VCG, 2 degrees maximum heel angle and 0.5 degrees initial heel angle

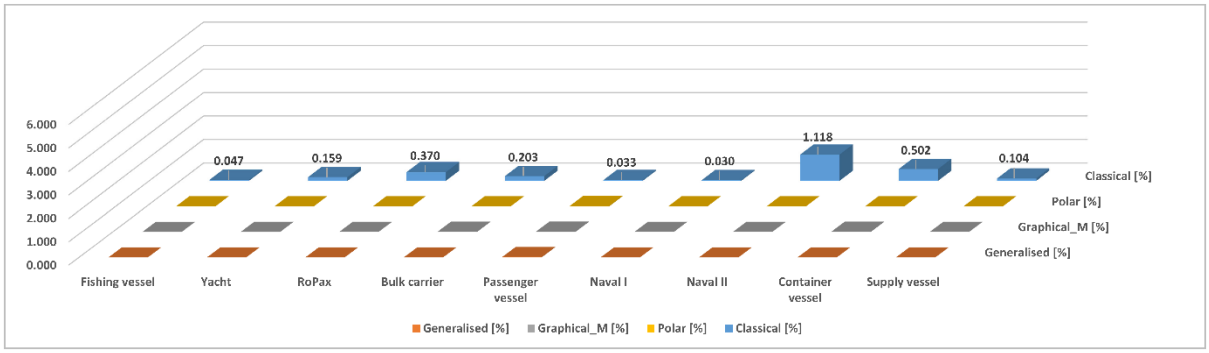

Fig. 17: Percentage error for VCG, 4 degrees maximum heel angle and 0.5 degrees initial heel angle

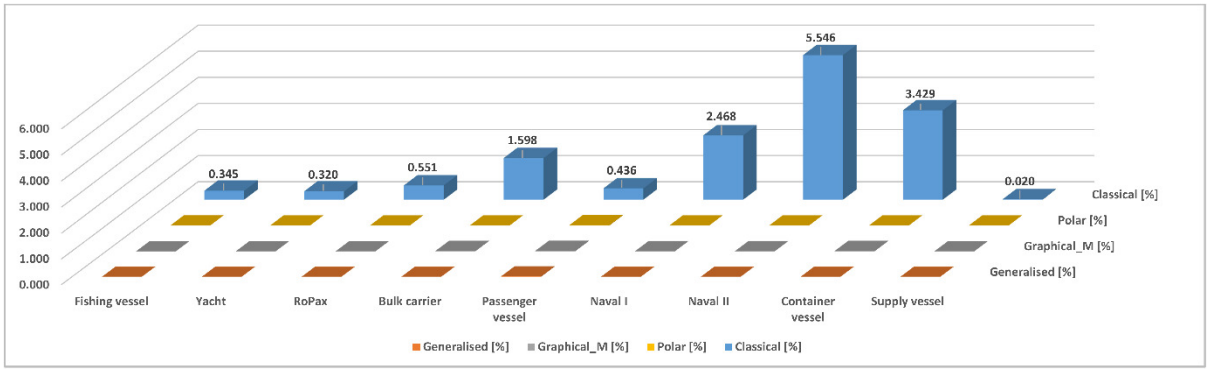

Fig. 18: Percentage error for VCG, 10 degrees maximum heel angle and 0.5 degrees initial heel angle

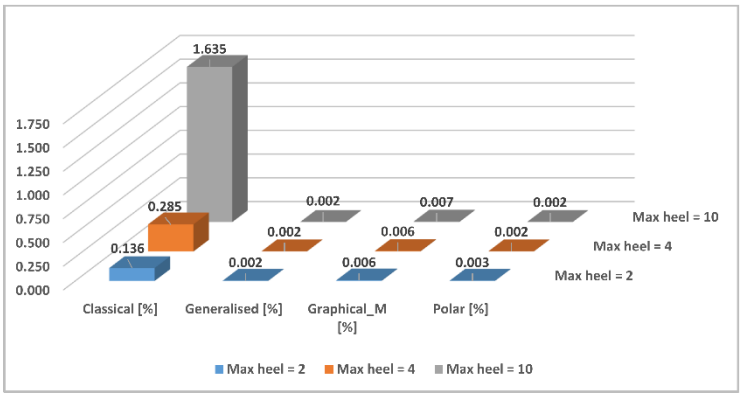

Fig. 19: Error potential averaged over vessel types, various heel angles and methods, 0.5 degrees initial heel

Finally, the cases with initial heel of 1 degree are presented. Again, a similar trend to that of the other initial heel angles is seen from Figures 20-23. As before, the *Classical* method is seen to be highly dependent on the heel angle magnitude, as the error increases significantly with larger heel angles, from 0.5-1% for the smaller heel angles to almost 5% for the larger heel angle. Similar to the initial heel of 0.5, the errors are again slightly reduced from the upright cases for several vessels.

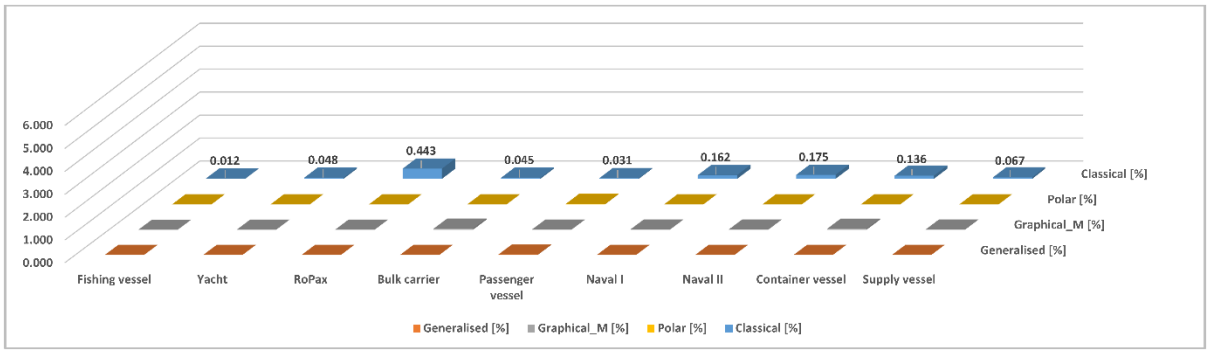

Fig. 20: Percentage error for VCG, 2 degree maximum heel angle and 1 degree initial heel angle

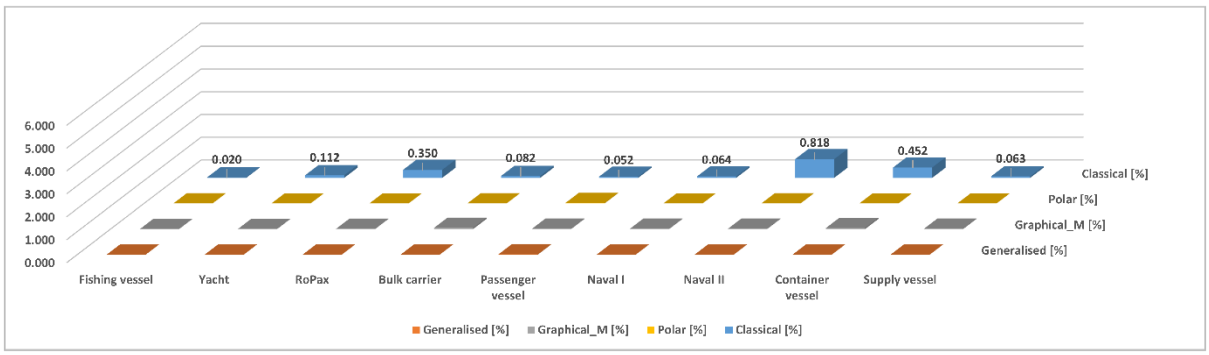

Fig. 21: Percentage error for VCG, 4 degree maximum heel angle and 1 degree initial heel angle

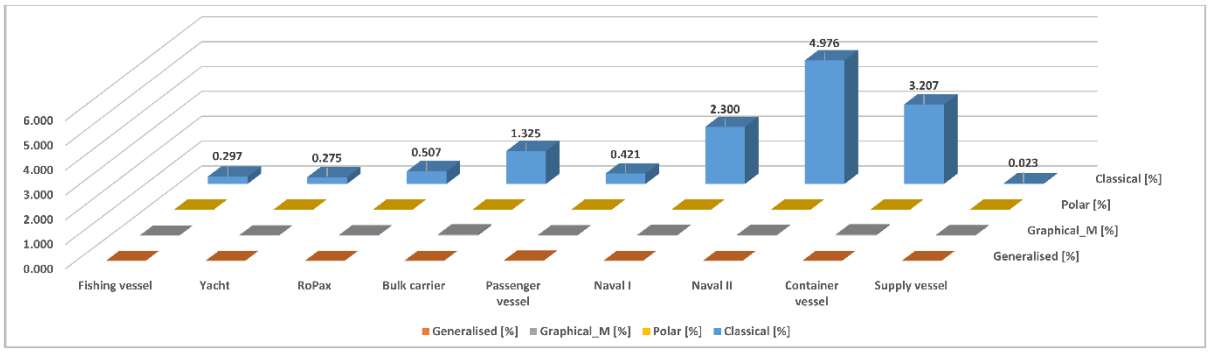

Fig. 22: Percentage error for VCG, 10 degree maximum heel angle and 1 degree initial heel angle

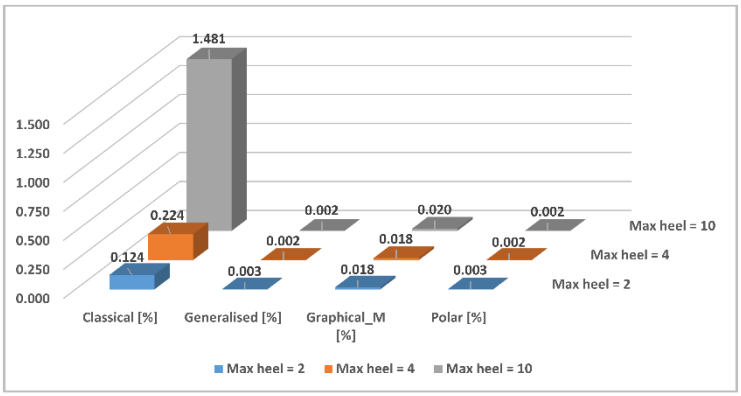

Fig. 23: Error potential averaged over vessel types, various heel angles and methods, 1 degree initial heel

To highlight the finding of decreased errors for larger initial heels, Figure 24 presents averaged errors for all vessel types, heel angles and methods for various initial heels. The decrease in error for the *Classical* method is clearly highlighted. The mathematical representation of the *Graphical* method, however, show a slight increase for initial heel angles.

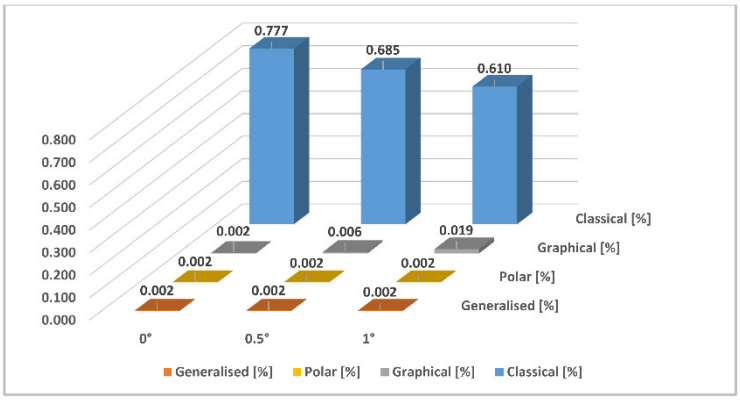

Fig. 24: Error potential averaged over vessel type, heel angles and methods, various initial heel angles

To highlight further the *Classical* method dependency on inclining heel angle, Figure 25 presents averaged errors for all vessel types, initial heel angles and methods for various inclining heels. The increase in error for larger inclining heel angles using the *Classical* method is again clearly highlighted.

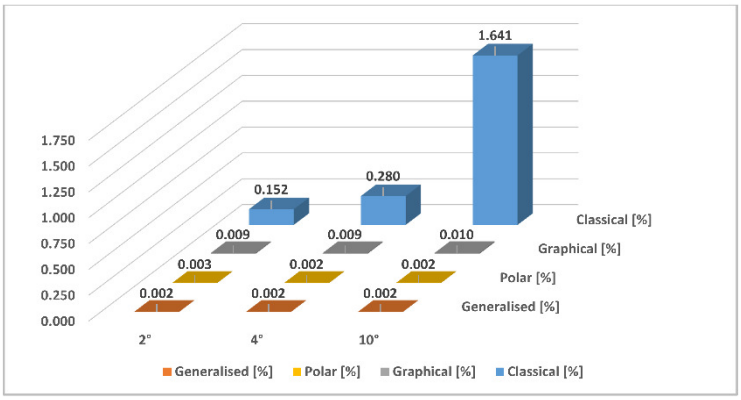

Fig. 25: Error potential averaged over vessel types, initial heel angles and methods, various inclining heel angles

The *Classical* method accuracy for the different vessel types is presented in Figure 26 for the various inclining heel angles. The Naval vessels and the Container vessel are showing highest error for all heel angles as would be expected due to their unconventional hull form with high fore- and aft flare and subsequent high change in waterplane area. For the vessel with the most onerous result, namely Naval II, the error is only 0.5% for 2 degrees heel angle, corresponding to 22 mm error in VCG. The error increases to 1.5% for 4 degrees of heel, corresponding to 75 mm error in VCG and to over 6% for 10 degrees of heel, corresponding to almost 300 mm error in VCG. It is further shown that a large error is obtained for large heel angles, even for the most conventional hull forms, such as the Bulk carrier, with almost 2% error, corresponding to 220 mm error in VCG. Some vessels that would be expected to give larger error, however, such as the Yacht and the RoPax, are showing smaller errors, despite their large change in waterplane area. The reason will be explained in the following.

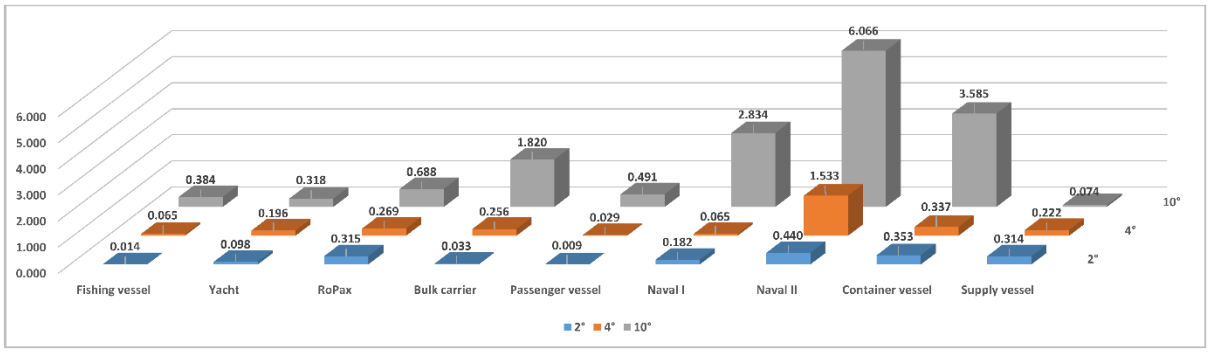

Fig. 26: Percentage-error potential for different vessel types, *Classical* method

Figure 27 presents the change in waterplane area, as well as arbitrary distance from the initial metacentre position when the vessel heels 0-20 degrees. The graph shows only the Fishing vessel for the sake of illustration but change in waterplane area for all vessels are presented in Appendix A. From the figure, it is clear that the change in metacentre position is proportional to the change in waterplane area as mentioned in the introduction. It would further be expected that the error potentials are proportional to the change in waterplane area as well. This is, however, not always the case as is seen in the low error potential obtained for the Yacht and RoPax, and is rather affected both by the movement direction as well as the movement magnitude. This is illustrated in Figure 28 below for the RoPax. Similar Graphs are presented in Appendix C for the remaining vessels.

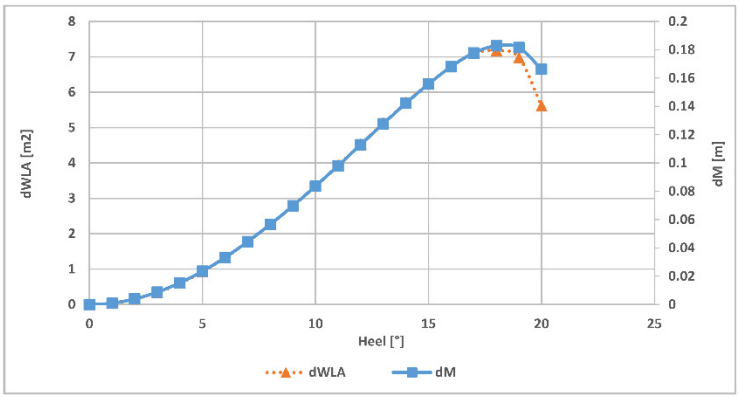

Fig. 27: Change in waterplane area and metacentre position for the fishing vessel

From Figure 28, large movement of the metacentre is shown due to change in the waterplane area. The error potential for the *Classical* method, as seen in Figure 26, is below 0.7%. Despite large movements of the metacentre, the position of the intersection with the centreline has not changed

much during the weight shifts and the trigonometric relationship for the calculation assumptions for the *Classical* method are still maintained. As long as the intersection point does not change, the assumption still holds and change in distance alone will not be decisive.

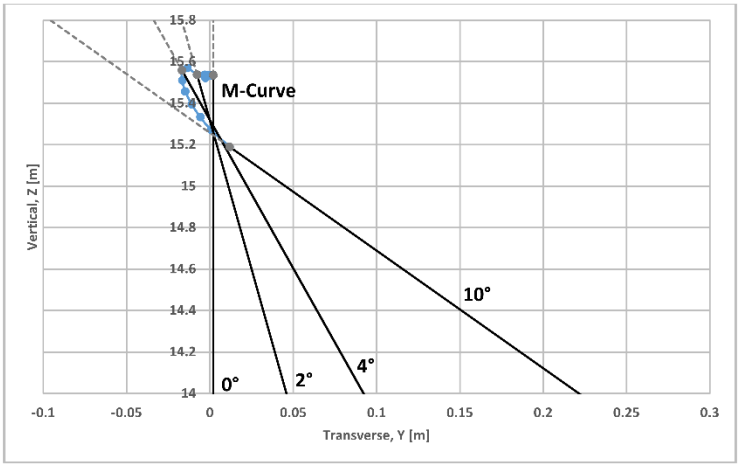

Fig. 28: Metacentre position for RoPax vessel

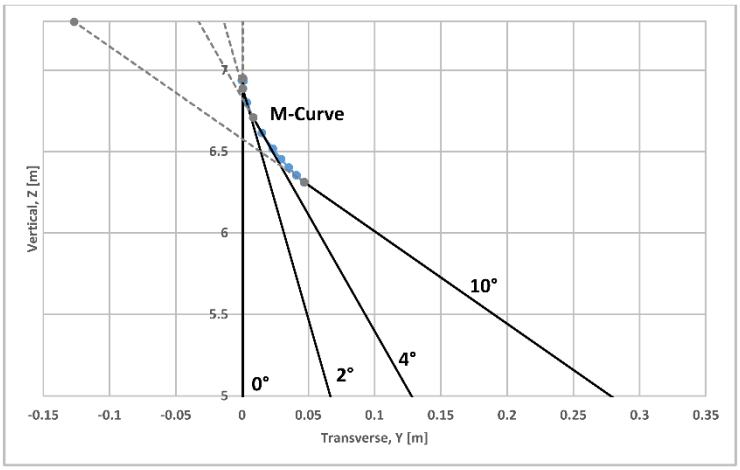

Fig. 29: Metacentre position for Naval II vessel

In Figure 29, a similar presentation is shown, but for the Naval II vessel. In this case, there are also large movements but in a direction that causes the intersection point with the centreline to be altered significantly, which is reflected in the larger error obtained as seen in Figure 27. This effect also seems to be the reason for the overall averaged reduction in error when applying initial heel angles to the *Classical* method as was highlighted in Figure 24. The *Classical* method does not depend on the TCG value itself as for the *Graphical* method but is rather dependent on the

combination of the metacentre movement direction and its magnitude. Large movement will not always result in large errors as long as the direction maintains the geometric relationship. Finally, in Figure 30, a summary of the errors obtained for the TCG calculation methods are presented. It is clear from the graph that all the methods are producing reliable results, with errors that can be disregarded.

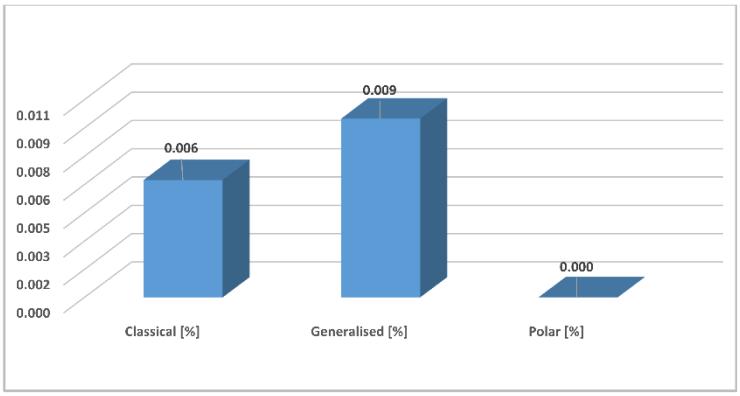

Fig. 30: Error potential for TCG, averaged over vessel types, initial heel and inclining heel, various methods

11.2 Extreme inclining angles and direct calculations

In the following, a more generalised approach was followed to assess the various methods. Extreme heel angles ranging from +/- 20 degrees were used, including initial heel angles ranging from 0-5 degrees. It is again important to note that such extreme heel angles are not practical for actual inclining experiments and are only included to put the various methods to the test. The methods were used to calculate the VCG values using their respective formulae directly rather than using a linear regression approach. To illustrate, the results from each method have been presented in Figures 31-34 for the Passenger vessel. Results for the remaining vessels are presented in Appendix B. As can be seen in the figures, all methods except the *Polar* method are affected by division by zero when the heel angle goes towards zero and the VCG result tend to infinity. As the *Polar* method is corrected for the initial KN_0 and heel angle φ_0, it will produce constant results for the VCG values for any angle of heel, φ_i, except for the initial heel, φ_0.

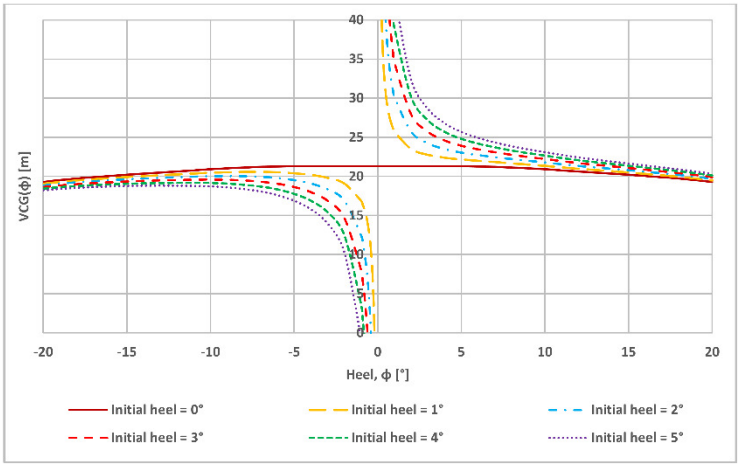

Fig. 31: Large heel angle incline for various initial heel angles, *Classical* method, direct calculation

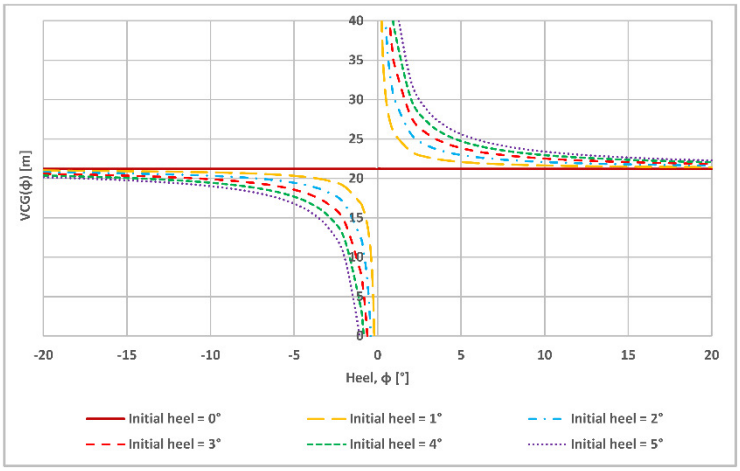

Fig. 32: Large heel angle incline for various initial heel angles, *Graphical* method, direct calculation

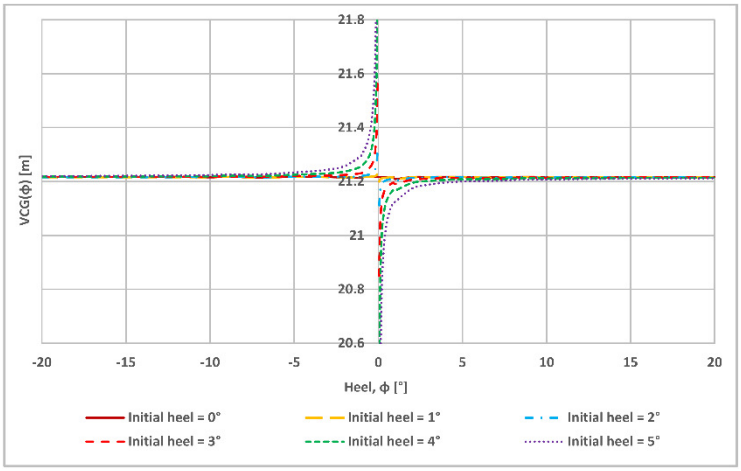

Fig. 33: Large heel angle incline for various initial heel angles, *Generalised* method, direct calculation

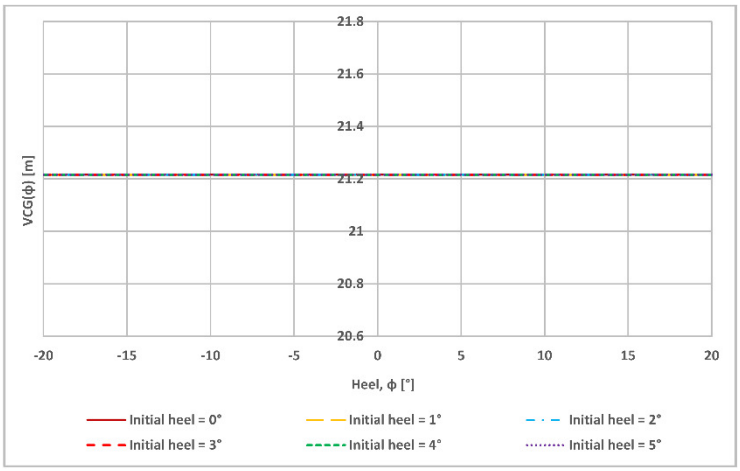

Fig. 34: Large heel angle incline for various initial heel angles, *Polar* method, direct calculation

11.3 Physical inclining experiment results and corrections

Resulting VCG values from applying the *Classical* method to *physical* inclining experiment readings are presented together with the corrections obtained using the error potentials in Table 3.

Table 3: Corrected VCG values obtained using error potentials for the *Classical* method

Vessel type	**VCG [m]**	**Correction [mm]**	$\boldsymbol{VCG_{corr}}$**[m]**
Fishing vessel	5.753	0.373	5.754
Yacht	3.747	4.207	3.752
RoPax	13.171	41.478	13.213
Bulk Carrier	11.632	2.789	11.634
Passenger Vessel	22.221	-3.084	22.218
Naval I	4.500	8.605	4.509
Naval II	4.934	-21.705	4.912
Container Vessel	17.228	60.813	17.288
Supply Vessel	7.592	7.897	7.600

From the table, it is clear that there are potential errors in the *physical* VCG values as a result of using the *Classical* method. The highest error is obtained for the RoPax, Naval II and Container vessel, with 41, 22 and 61 mm errors respectively. The VCG or the Naval II vessel is overestimated, while the VCG for the RoPax and Container vessels are underestimated. As these vessels have the highest potential underestimation, these have been used for checking their stability margins. As

both vessels have intact and damage stability limit-curves, these have been used to check margins. The worst-case loading conditions have been updated for the corrected lightweight VCG values and checked against the available stability margins from the limit curves as seen in Table 4. The stability margins have been exceeded with 11 mm for the Container vessel, while the RoPax vessel still has a 20 mm margin left.

Table 4: Worst case loading condition and stability margins

Vessel type	VCG [m]	Max VCG [m]	Margin [m]
Container Vessel	23.127	23.116	-0.011
RoPax	12.830	12.850	0.020

12. Concluding remarks

From the study detailed in the foregoing, it is clear that the various methods produce results with varying accuracy. In this section, concluding remarks for each method will be presented. Firstly, the *Classical* method will be discussed. As seen in the results, the *Classical* method produce viable results for the smallest applied heel angle of 2 degrees. For certain vessels, the error is almost three times as much for slightly larger heel angles of 4 degrees and almost ten times for larger heel angles of 10 degrees. It is clear that the method is highly dependent on the magnitude of the heel angle and could be unacceptable even for smaller heel angles for certain vessel types. This is particularly highlighted by the fact that the Container vessel exceeds the allowable stability limit curve when corrected for the error. Fortunately, most other vessels are overestimated, affecting only the vessels loading capacity. This, however, can be regarded as a safety factor. The limitations of the *Classical* method have been confirmed as it produces high errors for certain hull forms. This study shows further that large change in waterplane area does not necessarily mean large error in results as it is also affected by the direction of the movement. Care needs to be taken, when applying the *Classical* method, in terms of choosing loading conditions that result in low change in waterplane area, and use of smaller heel angles. A maximum angle of 2 degrees is recommended based on the derived

results. The *Graphical* method is shown to be working well for complete upright vessel for all vessel types and larger heel angles. It is, however, slightly more time consuming, considering that it requires to graphically draw all the steps in a Cad-software manually. It is further shown, that it can be very sensitive to the magnitude of the inclining heel angles chosen, making it difficult to apply graphically for smaller heel angles. The mathematical representation of the *Graphical* method produces better results for cases with initial heel angles as the linear regression accounts for the over-, and underestimation as mentioned earlier, and for the smaller heel angles. The linear regression further accounts for the fact that the formula does not consider initial heels, nor vessel asymmetry, and should therefore not be applied directly calculating an average VCG. The *Graphical* method limitation to initial heel angles is highlighted in Kanifolskyi & Konotopets (2016) but its limitation is stated to be $\pm$ 0.5 degrees heel. In this study, it seems that the method should be limited further, as the calculated results for 0.5 degree of initial heel angle show quite extensive errors. The *Generalised* method produces accurate results for all vessel types, heel angles and initial heel angles. The formula seems not to account entirely for the initial heel and asymmetry as discussed in the foregoing but this seems to be of less importance using the linear regression. The formula should therefore not be used to calculate the VCG directly using an averaged value. The formula is dependent on the correct calculation of the TCG using a third polynomial fit and may be slightly more time consuming than having a separate equation for calculating the TCG value directly. The *Polar* method seems to be the most general and mathematically correct as it accounts for any vessel asymmetry and for any initial heel angle. It also has two separate equations for VCG and TCG making them independent from each other. It is furthermore, the only method which produces constant results when calculating directly for any inclining heel angle during the weight shifts as it is not limited by division by zero. In the results presented in this study, theoretical values have been applied for KN and HZ since we have disregarded any external influences. In an actual inclining experiment, there are various uncertainties affecting the quality of the KN and HZ values applied in the equation. This will affect the results when applying direct calculations. It may, however, be

interesting to do further research on the matter, to see if reliable direct calculation results can be produced in actual inclining experiments, reducing the number of needed shifts from what is normal practice today. The *Classical* method works well for most vessel types as long it is applied correctly. It is a well-known fact that an *as inclined* loading conditions should be identified so that the waterplane area changes minimally. These additional measures are unnecessary when applying the other methods as they do not consider the metacentre in the equations. The other methods, especially the *Generalised* and the *Polar* method, produce very accurate results for any floating position of the vessel, in terms of draught, heel magnitude, and initial heel. This reduces the possibility of making mistakes and they are therefore more reliable than the *Classical* method. They are also more flexible due to their application using larger heel angles. Larger heel angles are better for smaller ships as smaller heel angles are easily disturbed by external influences such as waves and wind. Considering the results from this study, it may be time to *tear down the wall*-sided assumption represented by the *Classical* method and replace it with the better and more flexible methods. It is at least important for the industry to know that there are other and more reliable alternatives to the *Classical* method and this should be accounted for in the regulations and guidelines in use today.

13. References

Dunworth, 2013, “Up Against the Wall”, International Maritime Conference, Pacific 2013 IMC, Sidney, Australia.

Dunworth, 2014, “Back Against the Wall”, RINA Transactions (International Journal of Small Craft Technology), 2014, 156(B2), p. 99-106.

Dunworth, 2015, “Beyond the Wall”, Proceedings of the 12th International Conference on the Stability of Ships and Ocean Vehicles, 14-19 June 2015, Glasgow, UK.

Smith, Dunworth & Helmore, 2016, “Towards the Implementation of a Generalised Inclining Method for the Determination of the Centre of Gravity”, International Maritime Conference, Pacific 2015 IMC, Sidney, Australia.

Kanifolskyi & Konotopets, 2016, “The Graphical Method for Analysis of the Inclining Test”, Modern Information Technologies in the Sphere of Security and Defense No 3 (27)/2016, p. 37-39.

International Maritime Organization, 2009, “Reg. II-1/5 of SOLAS Consolidated Edition 2009”, as adopted in IMO Res. MSC 216(82)), 2006.

International Maritime Organization, 2000, “Reg. II/2.7 of the International Code of Safety for High-Speed Craft Code, 2008 Edition”, as adopted in IMO Res. MSC.97(73)

International Organization for Standardization, 1977, “Reg. III/9 of the Torremolinos International Convention for the Safety of Fishing Vessels, as modified by the 1993 Protocol (SFV/Torremolinos Convention)”.

International Organization for Standardization, 2013, “ISO 12217-2:2013 – Small craft – Stability and buoyancy assessment and categorization”.

International Maritime Organization, 2008, “Part B Annex I of the International Code on Intact Stability 2008”, as adopted in IMO Res. MSC.267(85), 2008.

International Association of Classification Societies, 1990, “IACS Rec.31 - Inclining test unified procedure”.

DNV GL, 2016, “DNVGL-CG-0157 - Stability documentation for approval, Annex I”.

International Maritime Organization, 2008, “Part B Annex I of the International Code on Intact Stability 2008”, as adopted in IMO Res. MSC.267(85), 2008.

Shakshober & Montgomery, 1967, “Analysis of the inclining experiment”, Hampton Road Section of the Society of Naval Architects and Marine Engineers.

Woodward, Rijsbergen, Hutchinson & Scott, 2016, “Uncertainty analysis procedure for the ship inclining experiment”, Ocean Engineering 114 (2016), p.79-86.

Appendix A: Change in waterplane area and metacentre position

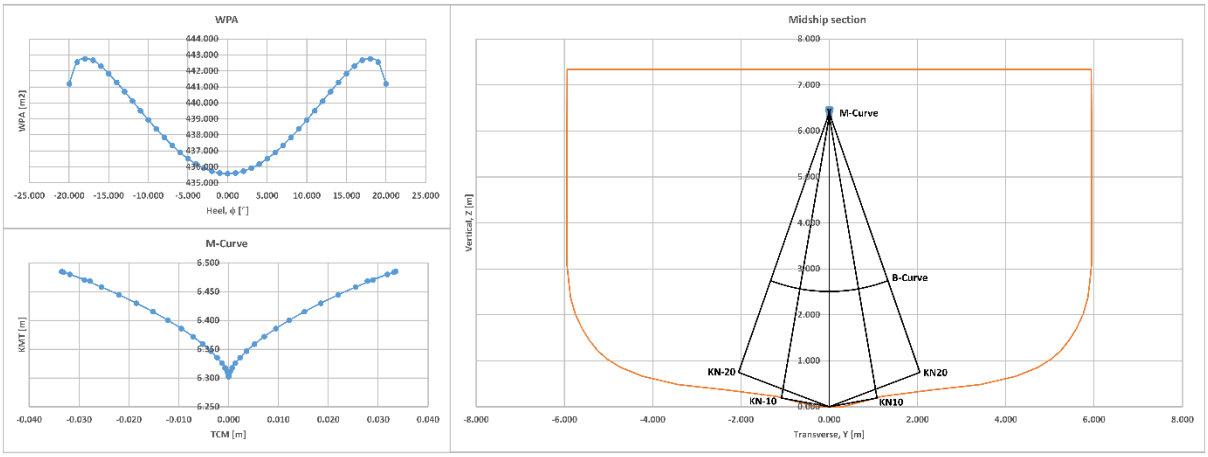

Fig. A.1: Change in waterplane area and metacentre position – Fishing Vessel

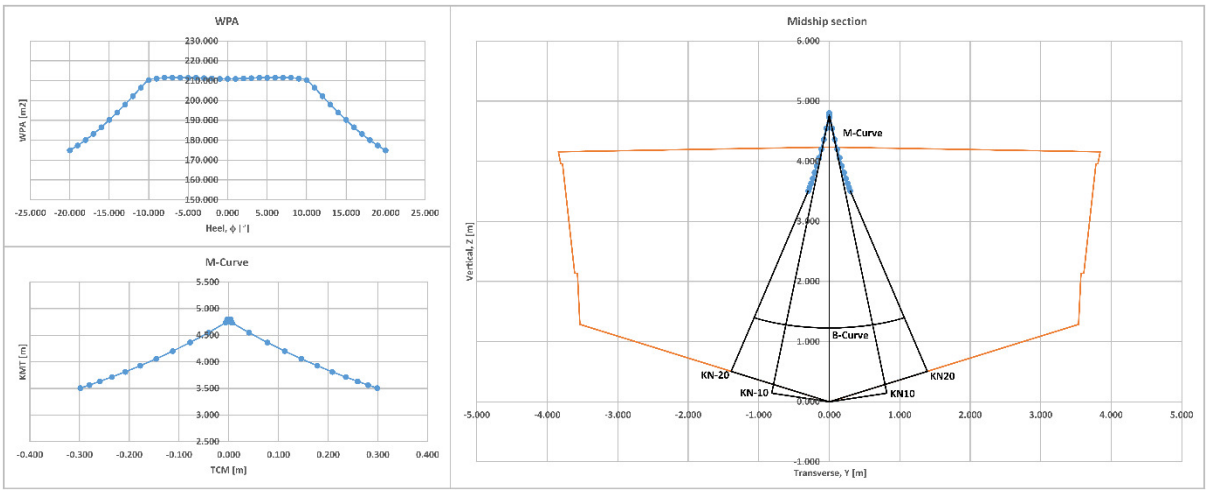

Fig. A.2: Change in waterplane area and metacentre position – Yacht

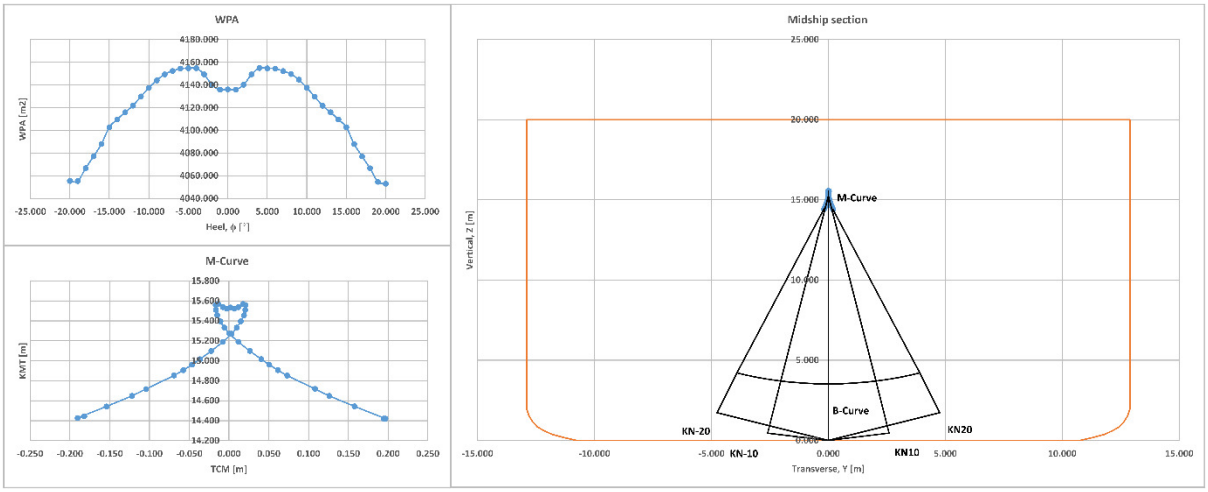

Fig. A.3: Change in waterplane area and metacentre position – RoPax

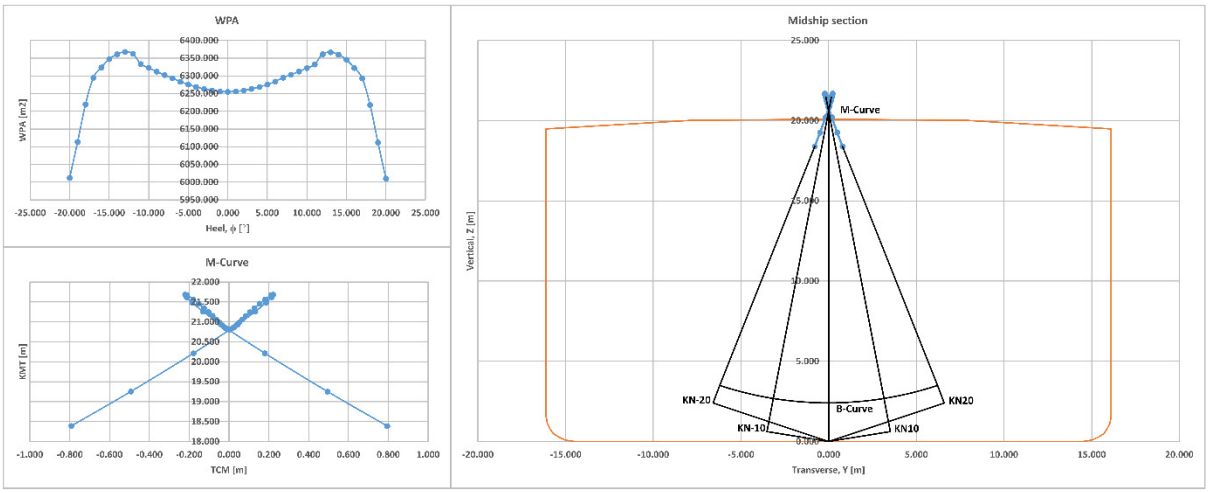

Fig. A.4: Change in waterplane area and metacentre position - Bulk carrier

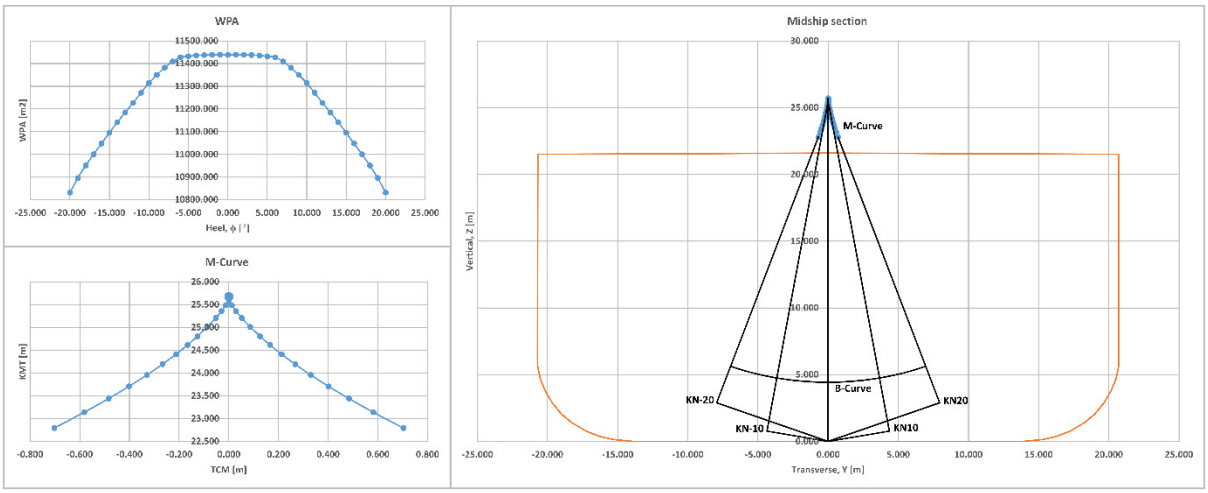

Fig. A.5: Change in waterplane area and metacentre position – Passenger vessel

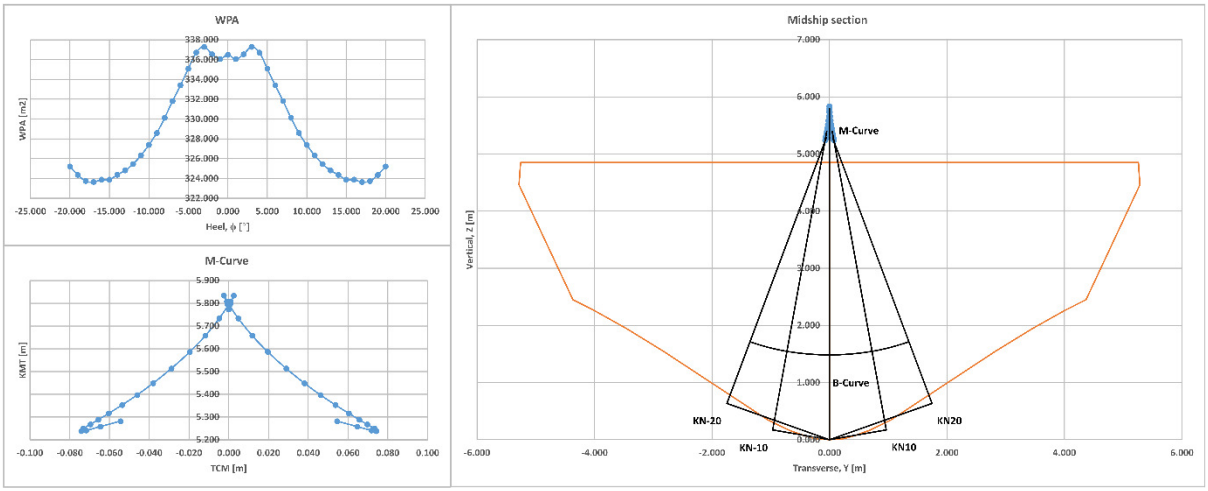

Fig. A.6: Change in waterplane area and metacentre position – Naval I

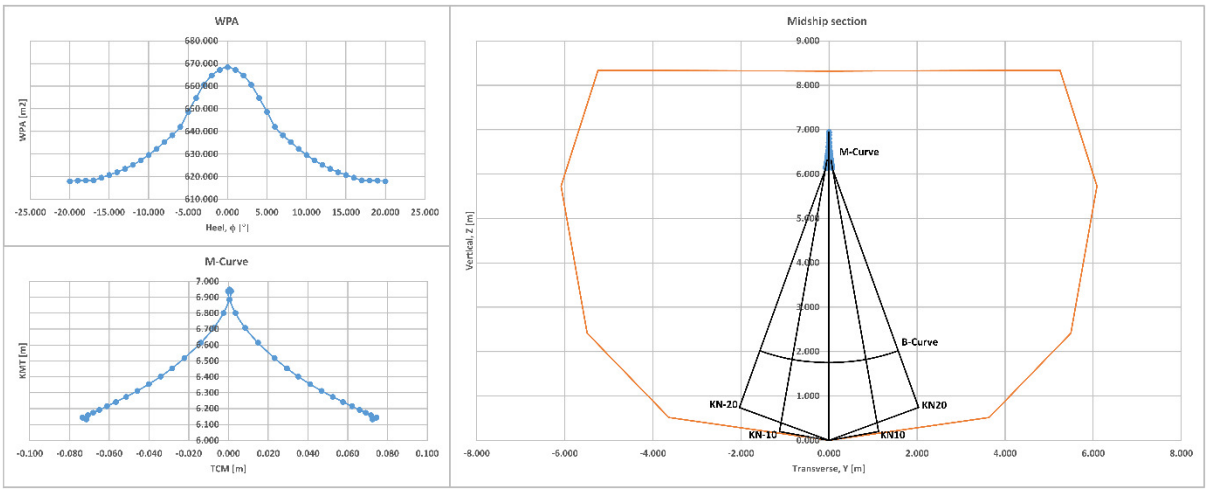

Fig. A.7: Change in waterplane area and metacentre position – Naval II

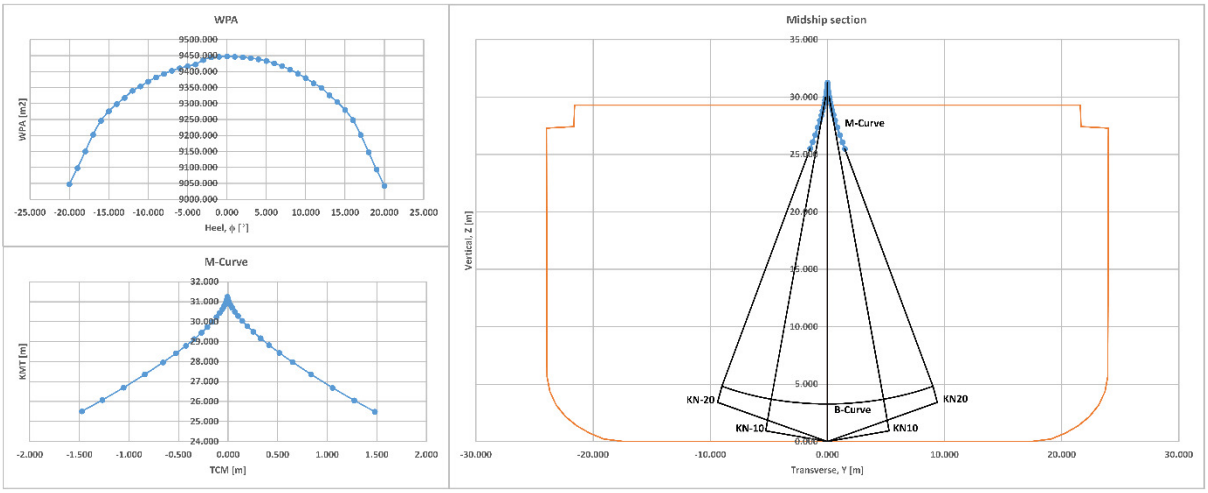

Fig. A.8: Change in waterplane area and metacentre position – Container vessel

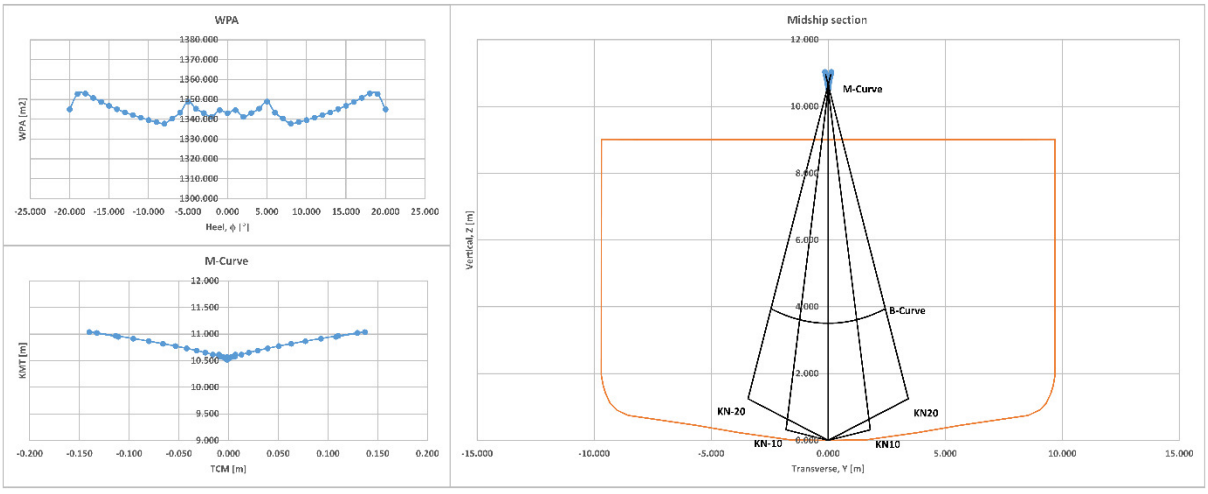

Fig. A.9: Change in waterplane area and metacentre position – Supply Vessel

Appendix B: Large heel incline with various initial heel angles

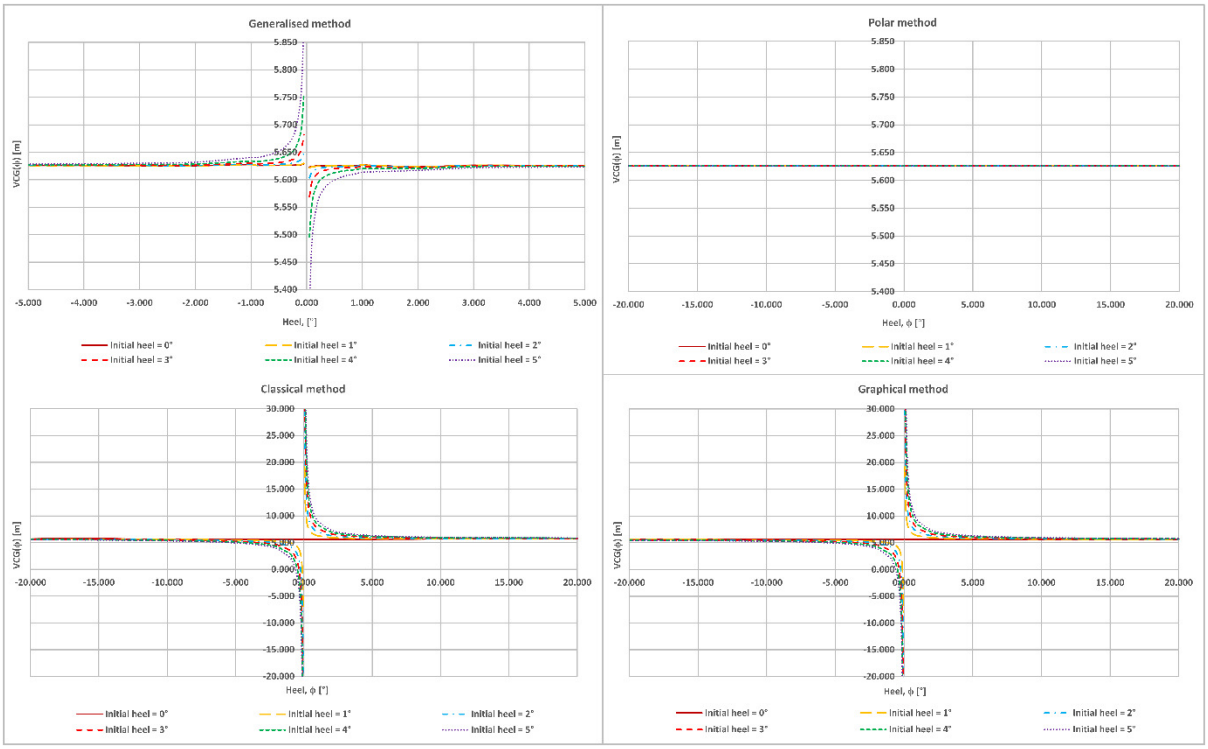

Fig. B.1: Large heel incline with various initial heel angles – Fishing Vessel

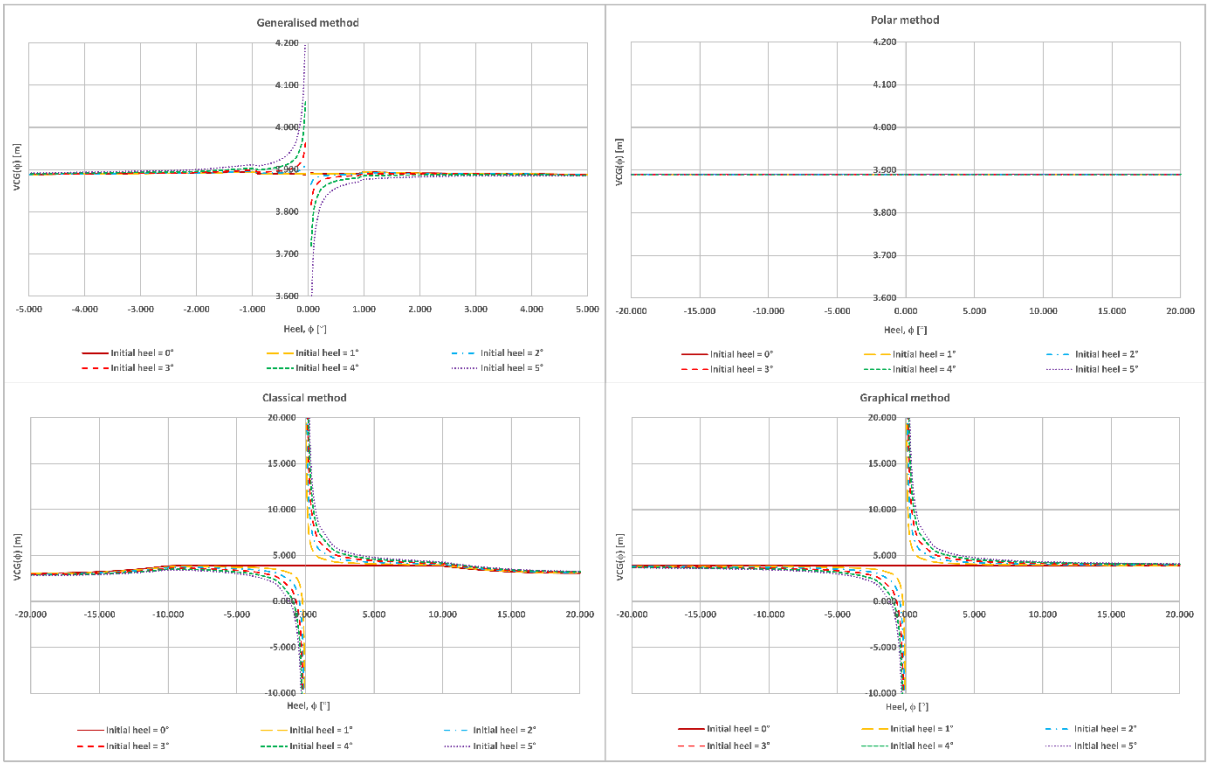

Fig. B.2: Large heel incline with various initial heel angles – Yacht

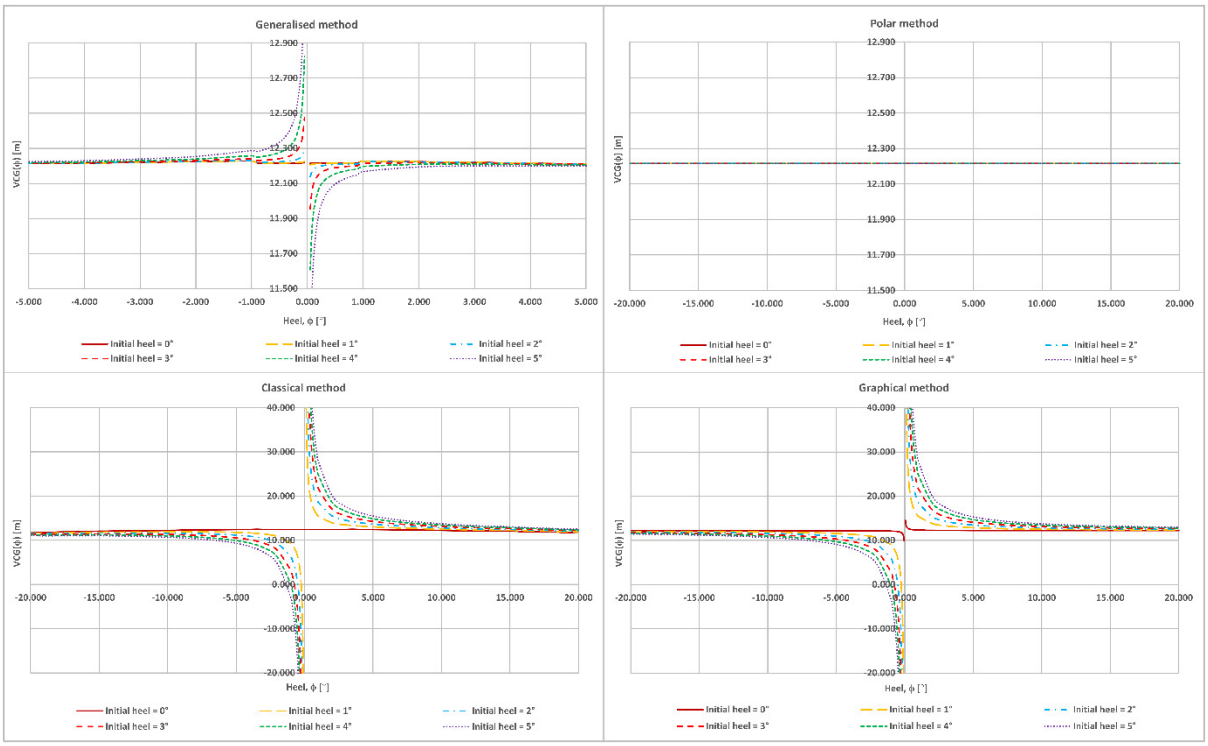

Fig. B.3: Large heel incline with various initial heel angles – RoPax

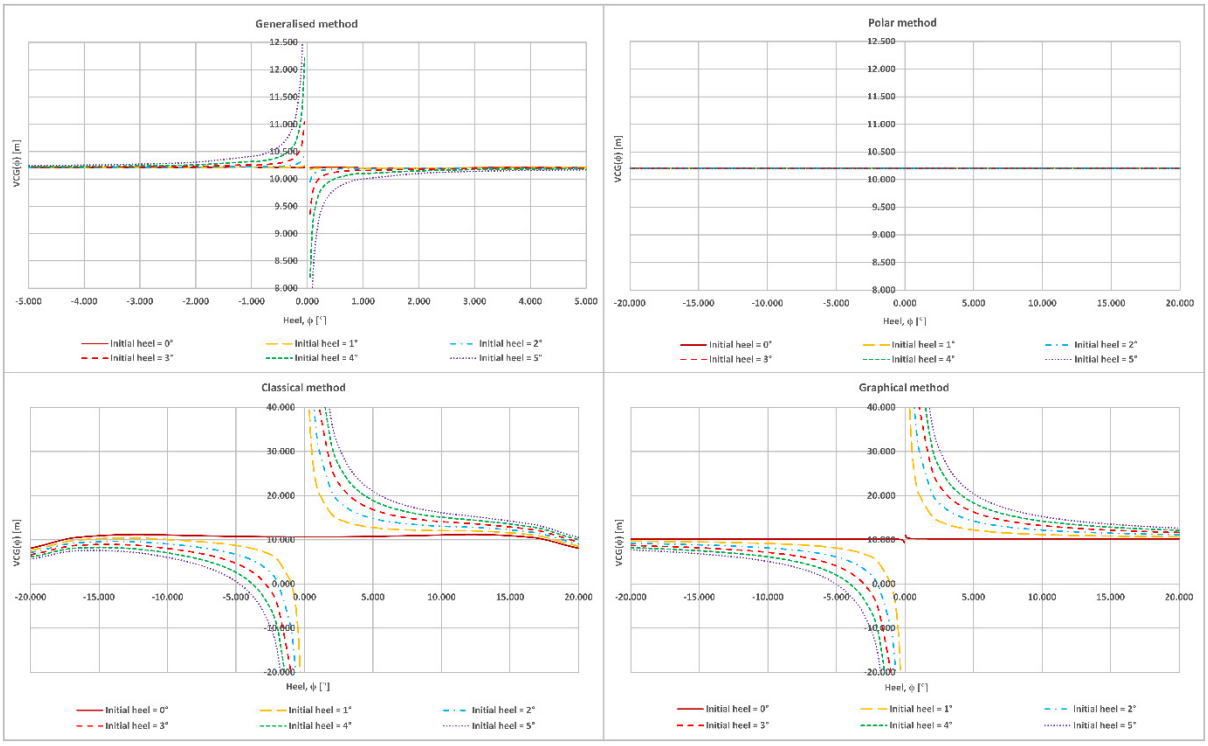

Fig. B.4: Large heel incline with various initial heel angles – Bulk Carrier

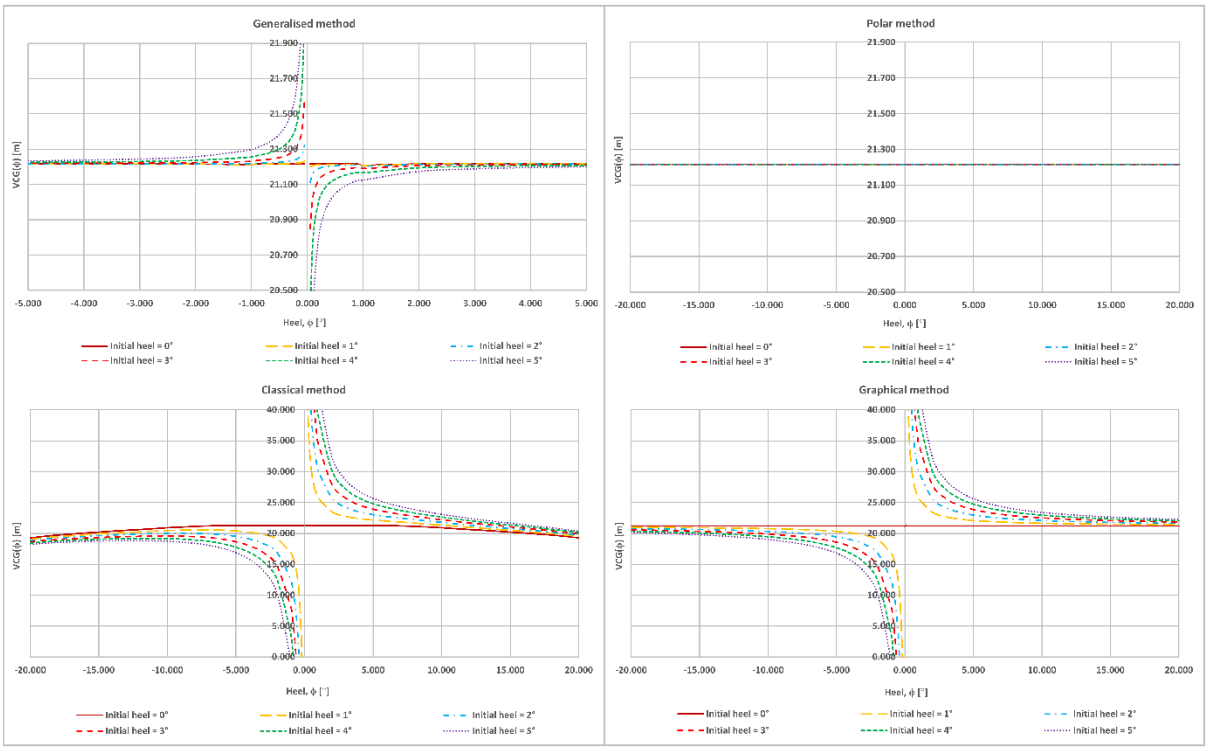

Fig. B.5: Large heel incline with various initial heel angles – Passenger Vessel

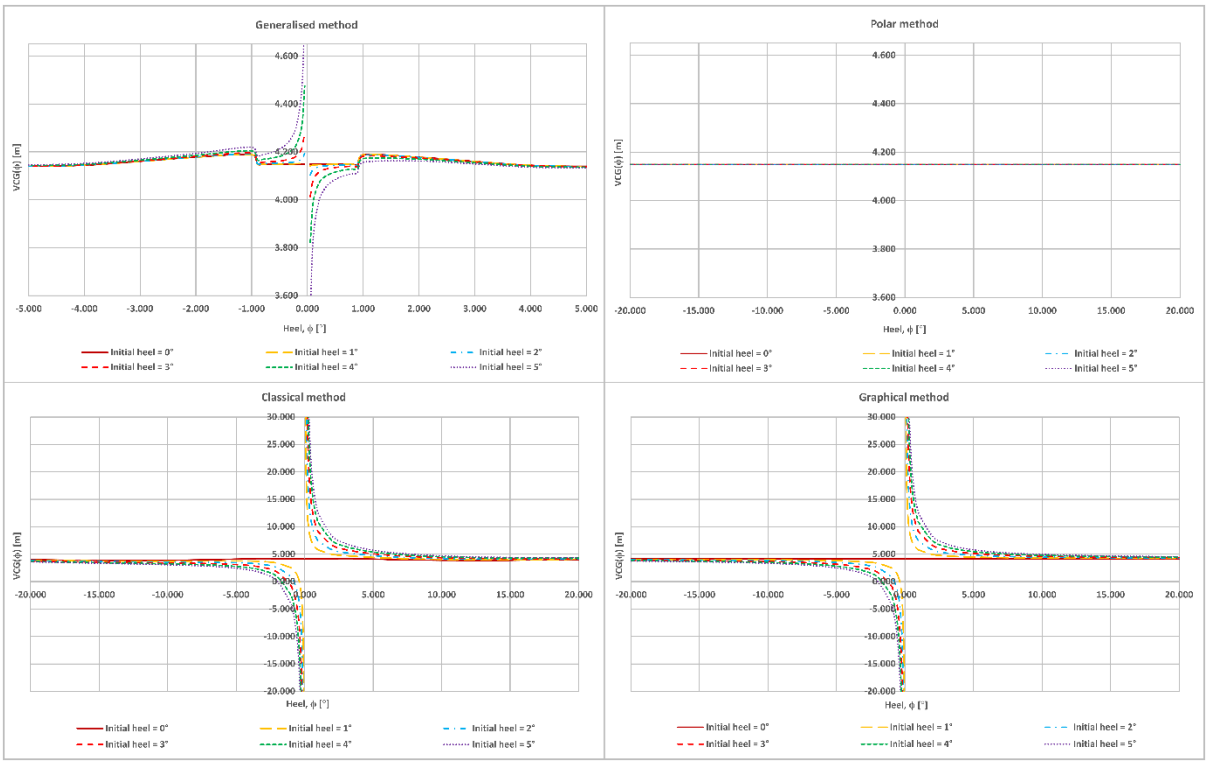

Fig. B.6: Large heel incline with various initial heel angles – Naval I

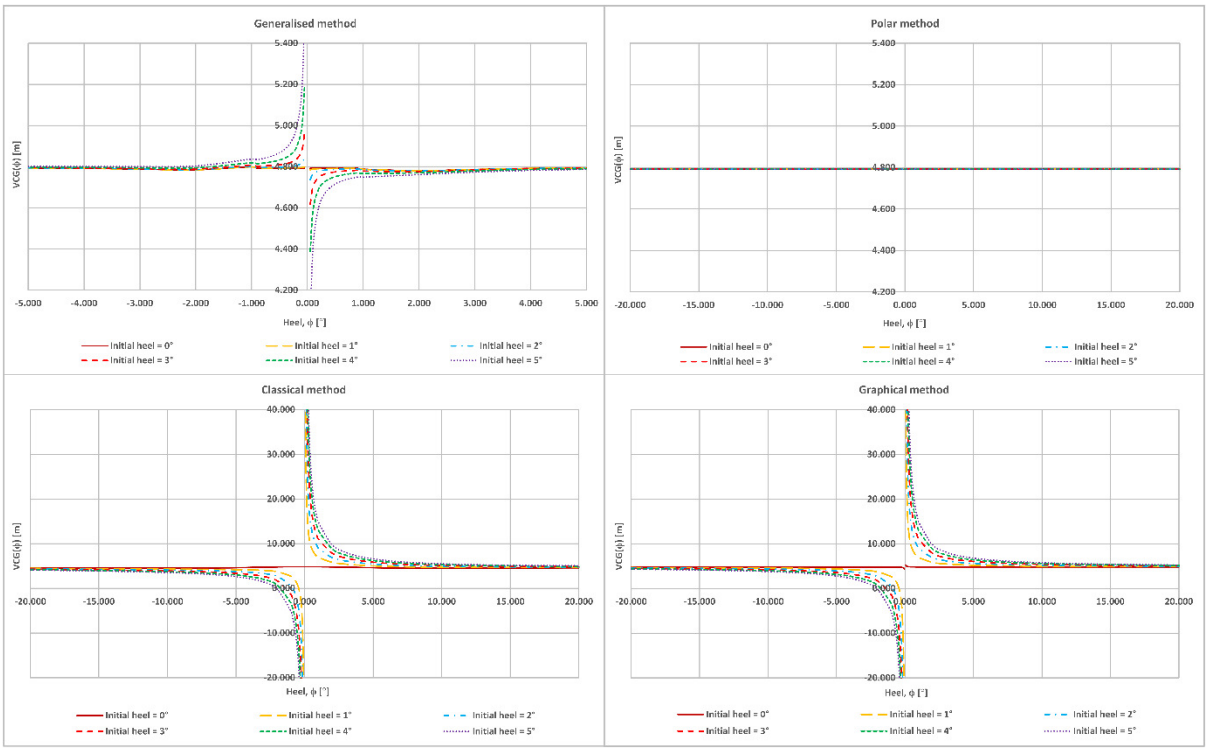

Fig. B.7: Large heel incline with various initial heel angles – Naval II

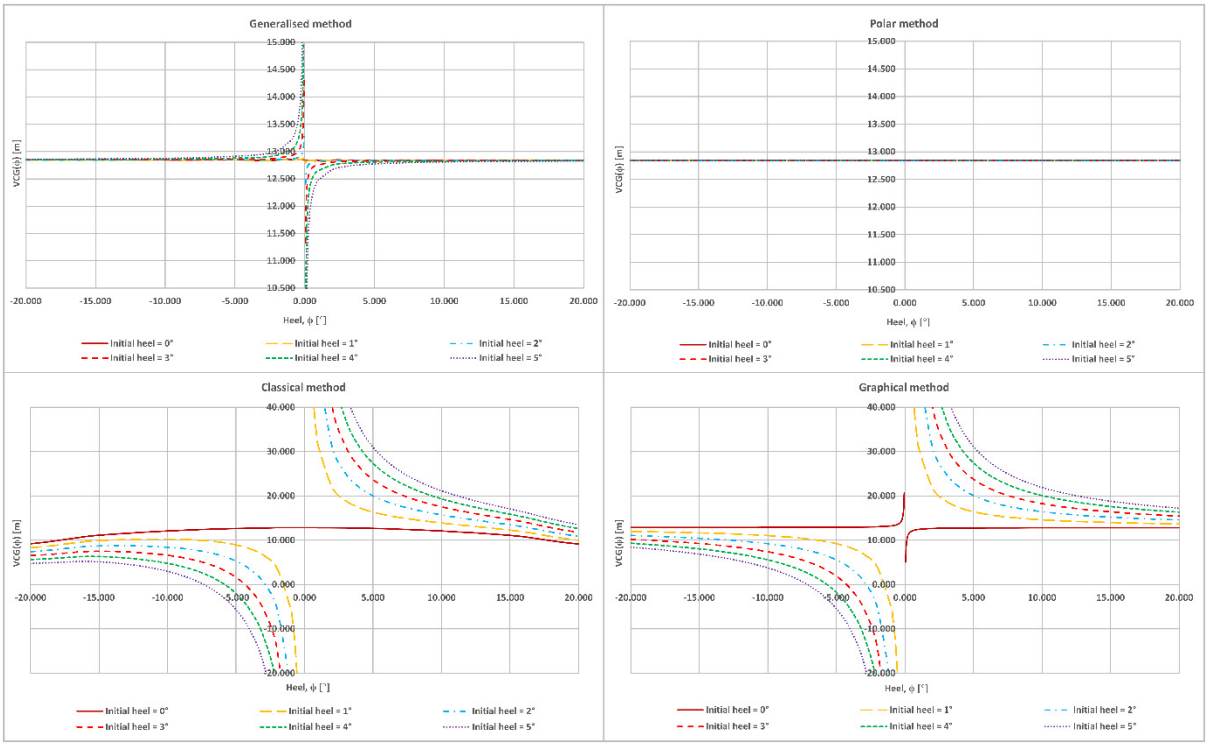

Fig. B.8: Large heel incline with various initial heel angles – Container Vessel

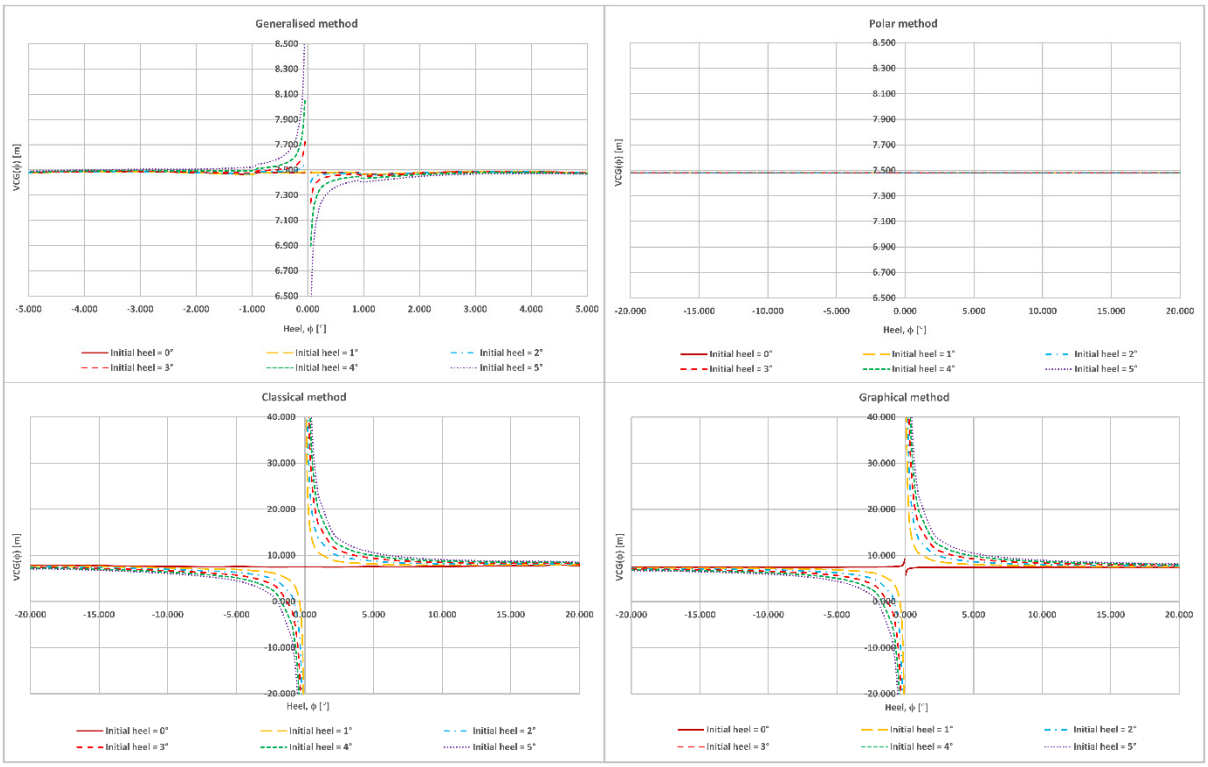

Fig. B.9: Large heel incline with various initial heel angles – Supply Vessel

Appendix C: Actual movement of the metacentre

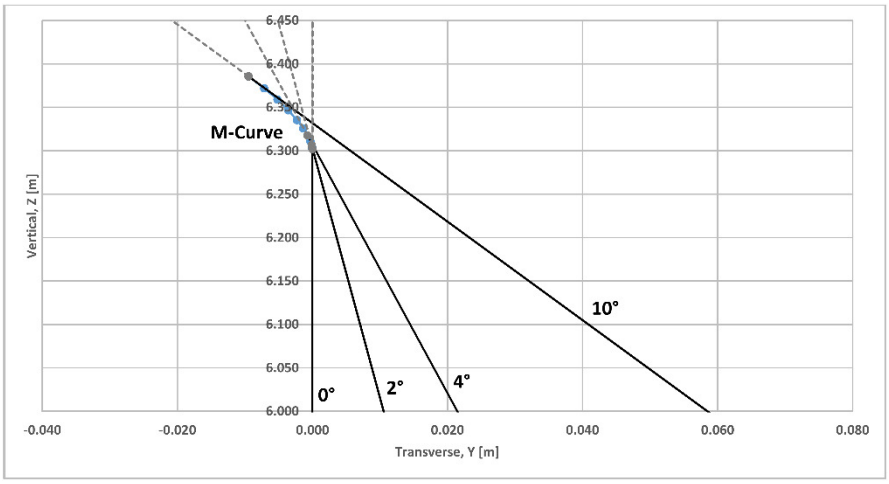

Fig. C.1: Large heel incline with various initial heel angles – Fishing Vessel

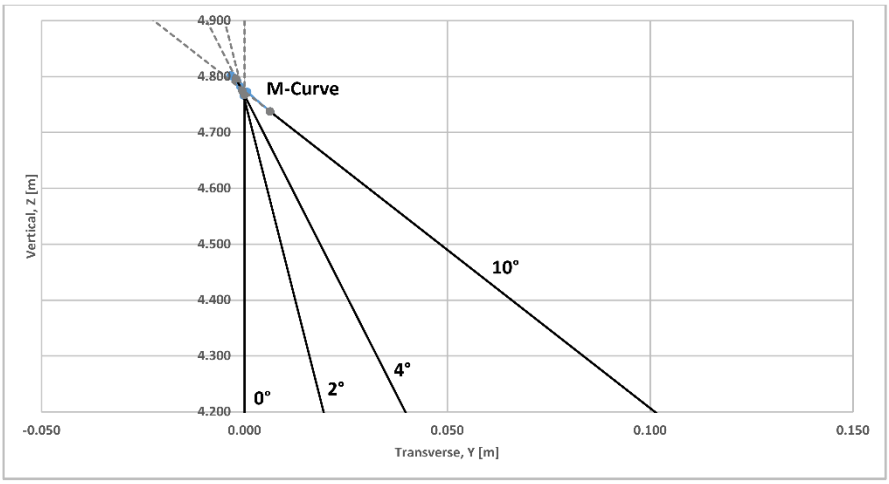

Fig. C.2: Large heel incline with various initial heel angles – Yacht

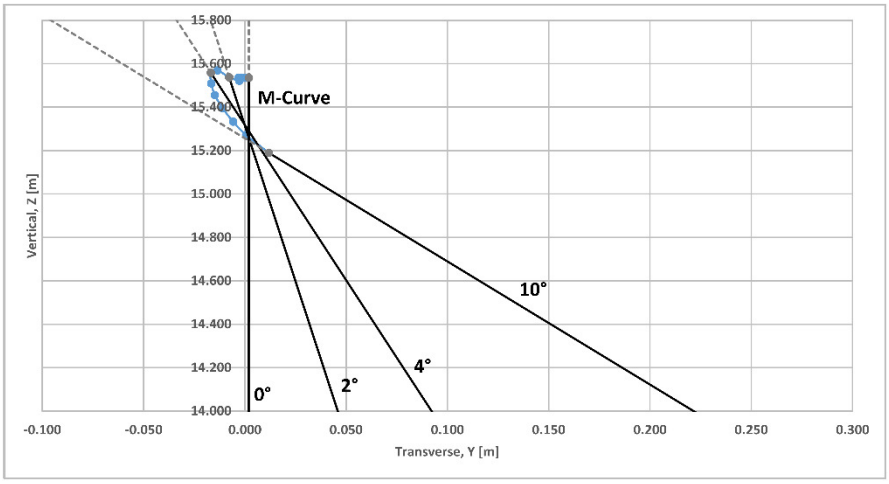

Fig. C.3: Large heel incline with various initial heel angles – RoPax

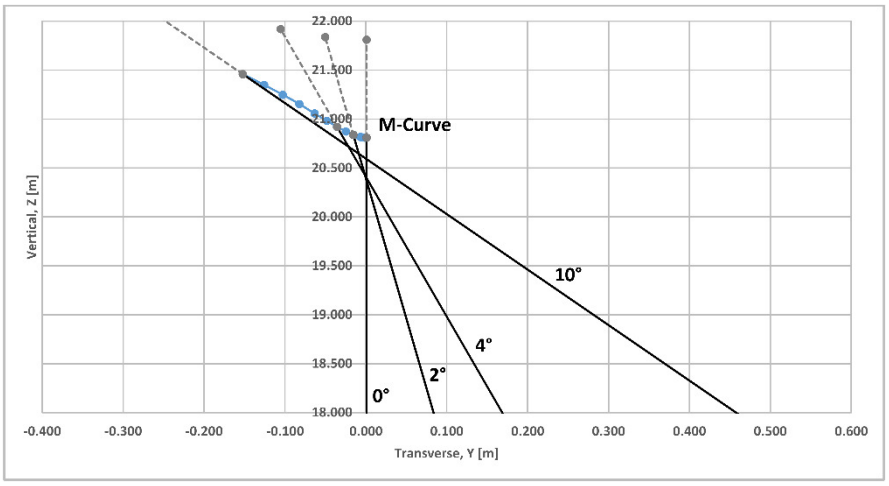

Fig. C.4: Large heel incline with various initial heel angles – Bulk Carrier

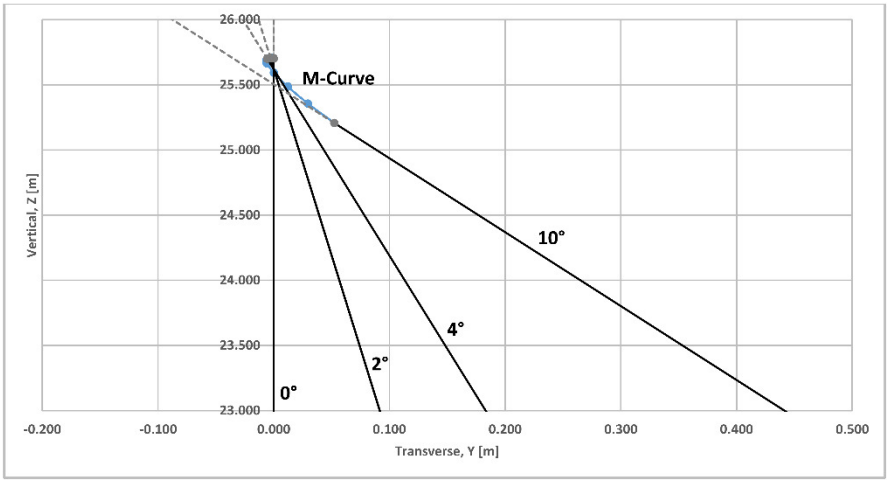

Fig. C.5: Large heel incline with various initial heel angles – Passenger Vessel

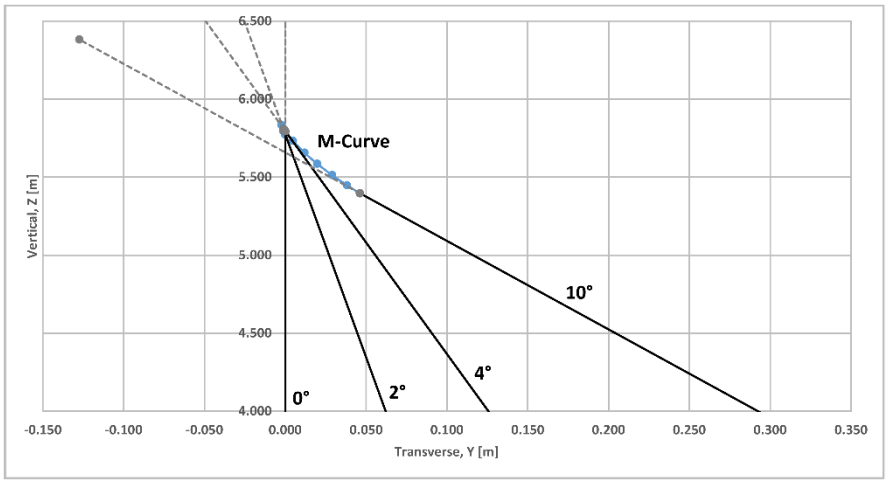

Fig. C.6: Large heel incline with various initial heel angles – Naval I

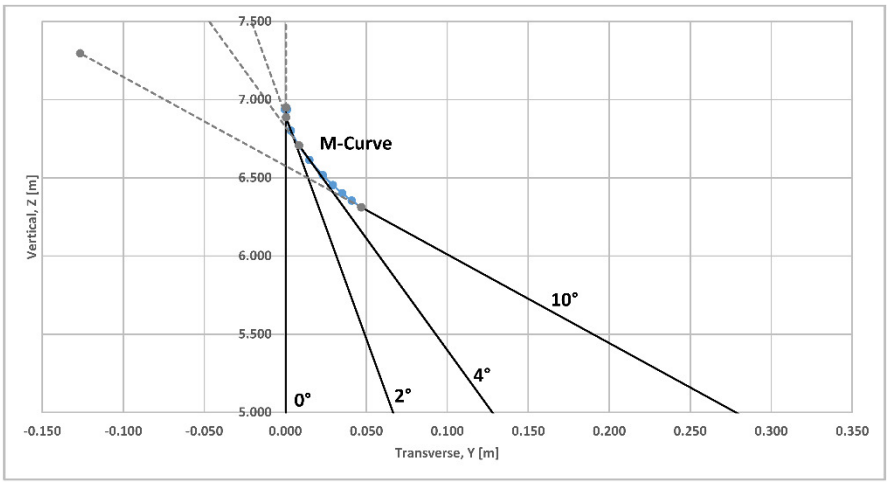

Fig. C.7: Large heel incline with various initial heel angles – Naval II

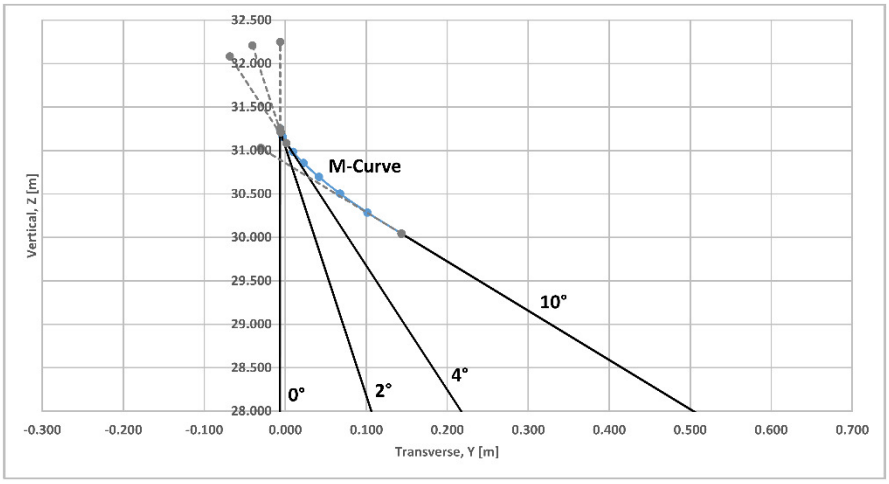

Fig. C.8: Large heel incline with various initial heel angles – Container Vessel

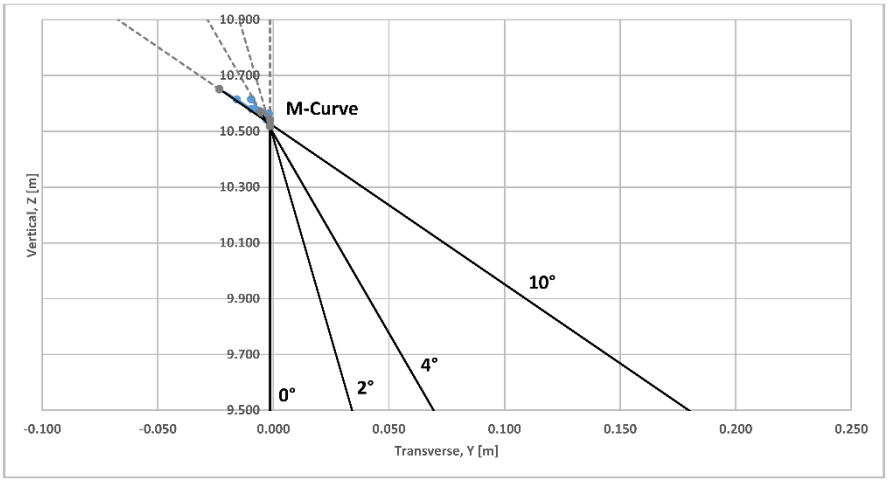

Fig. C.9: Large heel incline with various initial heel angles – Supply Vessel

Appendix D: Lines Plans

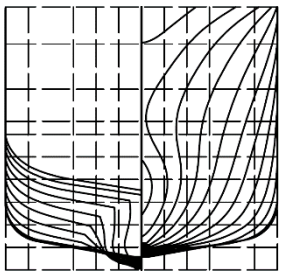

Fig. D.1: Lines – Fishing Vessel

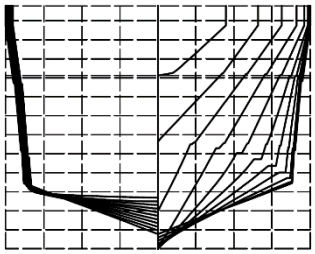

Fig. D.2: Lines – Yacht

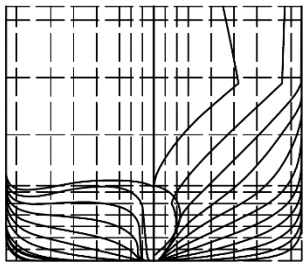

Fig. D.3: Lines – RoPax

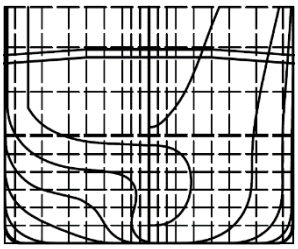

Fig. D.4: Lines – Bulk Carrier

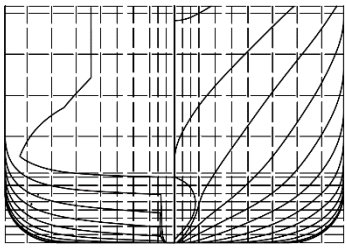

Fig. D.5: Lines – Passenger Vessel

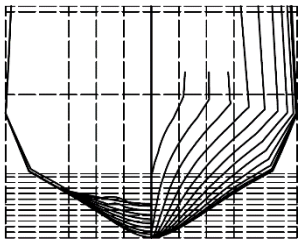

Fig. D.6: Lines – Naval I

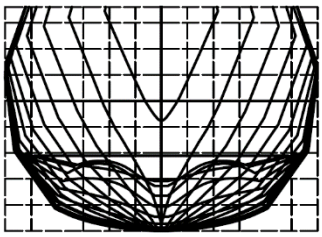

Fig. D.7: Lines – Naval II

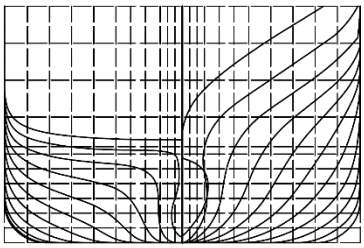

Fig. D.8: Lines – Container Vessel

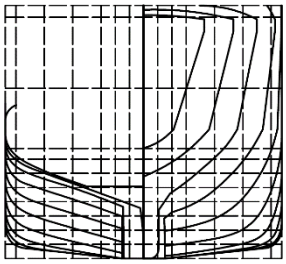

Fig. D.9: Lines – Supply Vessel

Appendix E: Detailed result - Technical incline

Table E.1: VCG obtained from technical incline, Max heel = 2, and Initial heel = 0

	Classical			Generalised			Graphical_M			Graphical_G			Polar			Actual
Vessel type	**VCG [m]**	**Error [mm]**	**Error [%]**	**VCG [m]**	**Error [mm]**	**Error [%]**	**VCG [m]**	**Error [mm]**	**Error [%]**	**VCG [m]**	**Error [mm]**	**Error [%]**	**VCG [m]**	**Error [mm]**	**Error [%]**	**VCG [m]**
Fishing Vessel	5.849	0.821	0.014	5.850	-0.071	-0.001	5.850	-0.071	-0.001	5.850	-0.078	-0.001	5.850	-0.071	-0.001	5.850
Yacht	3.846	3.784	0.098	3.850	0.005	0.000	3.850	0.005	0.000	3.850	0.004	0.000	3.850	0.005	0.000	3.850
RoPax	13.358	42.198	0.315	13.400	-0.042	0.000	13.400	-0.042	0.000	13.405	-4.950	-0.037	13.400	-0.041	0.000	13.400
Bulk Carrier	11.884	-3.903	-0.033	11.880	-0.104	-0.001	11.880	-0.104	-0.001	11.880	-0.424	-0.004	11.880	-0.104	-0.001	11.880
Passenger Vessel	22.222	-1.990	-0.009	22.224	-3.995	-0.018	22.224	-3.995	-0.018	22.224	-3.997	-0.018	22.224	-3.995	-0.018	22.220
Naval I	4.442	8.086	0.182	4.450	0.004	0.000	4.450	0.004	0.000	4.450	0.003	0.000	4.450	0.004	0.000	4.450
Naval II	4.871	-21.337	-0.440	4.850	-0.047	-0.001	4.850	-0.047	-0.001	4.850	-0.246	-0.005	4.850	-0.047	-0.001	4.850
Container Vessel	14.847	52.597	0.353	14.900	0.077	0.001	14.900	0.077	0.001	14.910	-9.721	-0.065	14.900	0.079	0.001	14.900
Supply Vessel	7.476	23.555	0.314	7.500	-0.022	0.000	7.500	-0.022	0.000	7.503	-2.554	-0.034	7.500	-0.022	0.000	7.500
	Pos. Avg.:	17.586	0.195	Pos. Avg.:	0.485	0.002	Pos. Avg.:	0.485	0.002	Pos. Avg.:	2.442	0.018	Pos. Avg.:	0.485	0.002	

TableE.2: VCG obtained from technical incline, Max heel = 4, and Initial heel = 0

	Classical			Generalised			Graphical_M			Graphical_G			Polar			Actual
Vessel type	**VCG [m]**	**Error [mm]**	**Error [%]**	**VCG [m]**	**Error [mm]**	**Error [%]**	**VCG [m]**	**Error [mm]**	**Error [%]**	**VCG [m]**	**Error [mm]**	**Error [%]**	**VCG [m]**	**Error [mm]**	**Error [%]**	**VCG [m]**
Fishing Vessel	5.846	3.828	0.065	5.850	-0.066	-0.001	5.850	-0.066	-0.001	5.850	-0.069	-0.001	5.850	-0.066	-0.001	5.850
Yacht	3.842	7.563	0.196	3.850	0.009	0.000	3.850	0.009	0.000	3.850	0.007	0.000	3.850	0.009	0.000	3.850
RoPax	13.364	36.014	0.269	13.400	-0.034	0.000	13.400	-0.034	0.000	13.401	-1.266	-0.009	13.400	-0.033	0.000	13.400
Bulk Carrier	11.850	30.423	0.256	11.880	-0.057	0.000	11.880	-0.057	0.000	11.880	-0.153	-0.001	11.880	-0.057	0.000	11.880
Passenger Vessel	22.226	-6.435	-0.029	22.224	-3.983	-0.018	22.224	-3.983	-0.018	22.224	-3.988	-0.018	22.224	-3.983	-0.018	22.220
Naval I	4.453	-2.893	-0.065	4.450	0.017	0.000	4.450	0.017	0.000	4.450	0.012	0.000	4.450	0.017	0.000	4.450
Naval II	4.924	-74.333	-1.533	4.850	-0.034	-0.001	4.850	-0.034	-0.001	4.850	-0.098	-0.002	4.850	-0.034	-0.001	4.850
Container Vessel	14.950	-50.186	-0.337	14.900	0.062	0.000	14.900	0.062	0.000	14.902	-2.378	-0.016	14.900	0.065	0.000	14.900
Supply Vessel	7.483	16.633	0.222	7.500	-0.011	0.000	7.500	-0.011	0.000	7.501	-0.656	-0.009	7.500	-0.010	0.000	7.500
	Pos. Avg.:	25.368	0.330	Pos. Avg.:	0.475	0.002	Pos. Avg.:	0.475	0.002	Pos. Avg.:	0.959	0.006	Pos. Avg.:	0.475	0.002	

Table E.3: VCG obtained from technical incline, Max heel = 10, and Initial heel = 0

	Classical			Generalised			Graphical_M			Graphical_G			Polar			Actual
Vessel type	**VCG [m]**	**Error [mm]**	**Error [%]**	**VCG [m]**	**Error [mm]**	**Error [%]**	**VCG [m]**	**Error [mm]**	**Error [%]**	**VCG [m]**	**Error [mm]**	**Error [%]**	**VCG [m]**	**Error [mm]**	**Error [%]**	**VCG [m]**
Fishing Vessel	5.828	22.442	0.384	5.850	-0.060	-0.001	5.850	-0.060	-0.001	5.850	-0.060	-0.001	5.850	-0.060	-0.001	5.850
Yacht	3.838	12.237	0.318	3.850	-0.005	0.000	3.850	-0.005	0.000	3.850	0.002	0.000	3.850	-0.005	0.000	3.850
RoPax	13.492	-92.133	-0.688	13.400	-0.029	0.000	13.400	-0.029	0.000	13.400	-0.213	-0.002	13.400	-0.031	0.000	13.400
Bulk Carrier	11.664	216.196	1.820	11.880	0.088	0.001	11.880	0.088	0.001	11.880	0.044	0.000	11.880	0.087	0.001	11.880
Passenger Vessel	22.329	-109.016	-0.491	22.224	-3.960	-0.018	22.224	-3.960	-0.018	22.224	-3.967	-0.018	22.224	-3.960	-0.018	22.220
Naval I	4.576	-126.094	-2.834	4.450	0.021	0.000	4.450	0.021	0.000	4.450	0.023	0.001	4.450	0.021	0.000	4.450
Naval II	5.144	-294.190	-6.066	4.850	-0.003	0.000	4.850	-0.003	0.000	4.850	-0.024	0.000	4.850	-0.003	0.000	4.850
Container Vessel	15.434	-534.098	-3.585	14.900	0.040	0.000	14.900	0.040	0.000	14.900	-0.415	-0.003	14.900	0.049	0.000	14.900
Supply Vessel	7.494	5.585	0.074	7.500	0.005	0.000	7.500	0.005	0.000	7.500	-0.122	-0.002	7.500	0.007	0.000	7.500
	Pos. Avg.:	156.888	1.806	Pos. Avg.:	0.468	0.002	Pos. Avg.:	0.468	0.002	Pos. Avg.:	0.541	0.003	Pos. Avg.:	0.469	0.002	

TableE.4: VCG obtained from technical incline, Max heel = 2, and Initial heel = 0.5

	Classical			Generalised			Graphical_M			Graphical_G			Polar			Actual
Vessel type	**VCG [m]**	**Error [mm]**	**Error [%]**	**VCG [m]**	**Error [mm]**	**Error [%]**	**VCG [m]**	**Error [mm]**	**Error [%]**	**VCG [m]**	**Error [mm]**	**Error [%]**	**VCG [m]**	**Error [mm]**	**Error [%]**	**VCG [m]**
Fishing Vessel	5.850	0.379	0.006	5.850	-0.083	-0.001	5.850	-0.024	0.000	5.926	-76.487	-1.307	5.850	-0.083	-0.001	5.850
Yacht	3.847	2.934	0.076	3.850	0.005	0.000	3.850	0.071	0.002	3.936	-85.837	-2.230	3.850	0.005	0.000	3.850
RoPax	13.336	64.292	0.480	13.400	-0.020	0.000	13.400	0.259	0.002	13.778	-377.611	-2.818	13.400	-0.040	0.000	13.400
Bulk Carrier	11.877	2.848	0.024	11.880	-0.116	-0.001	11.879	1.392	0.012	8.008	3871.717	32.590	11.880	-0.128	-0.001	11.880
Passenger Vessel	22.223	-3.083	-0.014	22.224	-3.986	-0.018	22.224	-3.632	-0.016	22.676	-455.665	-2.051	22.224	-3.986	-0.018	22.220
Naval I	4.441	8.510	0.191	4.450	0.003	0.000	4.450	0.153	0.003	4.639	-189.484	-4.258	4.450	0.003	0.000	4.450
Naval II	4.860	-9.861	-0.203	4.850	-0.050	-0.001	4.850	0.118	0.002	5.051	-200.762	-4.139	4.850	-0.054	-0.001	4.850
Container Vessel	14.919	-18.508	-0.124	14.900	0.015	0.000	14.898	1.726	0.012	16.982	-2081.986	-13.973	14.900	0.088	0.001	14.900
Supply Vessel	7.492	7.791	0.104	7.500	-0.031	0.000	7.500	0.218	0.003	7.800	-299.698	-3.996	7.500	-0.017	0.000	7.500
	Pos. Avg.:	13.134	0.136	Pos. Avg.:	0.479	0.002	Pos. Avg.:	0.844	0.006	Pos. Avg.:	848.805	7.485	Pos. Avg.:	0.489	0.003	

Table E.5: VCG obtained from technical incline, Max heel = 4, and Initial heel = 0.5

	Classical			Generalised			Graphical_M			Graphical_G			Polar			Actual
Vessel type	**VCG [m]**	**Error [mm]**	**Error [%]**	**VCG [m]**	**Error [mm]**	**Error [%]**	**VCG [m]**	**Error [mm]**	**Error [%]**	**VCG [m]**	**Error [mm]**	**Error [%]**	**VCG [m]**	**Error [mm]**	**Error [%]**	**VCG [m]**
Fishing Vessel	5.847	2.723	0.047	5.850	-0.074	-0.001	5.850	-0.016	0.000	6.001	-151.478	-2.589	5.850	-0.074	-0.001	5.850
Yacht	3.844	6.110	0.159	3.850	0.008	0.000	3.850	0.073	0.002	4.019	-169.247	-4.396	3.850	0.008	0.000	3.850
RoPax	13.350	49.604	0.370	13.400	-0.015	0.000	13.400	0.269	0.002	14.158	-758.095	-5.657	13.400	-0.036	0.000	13.400
Bulk Carrier	11.856	24.079	0.203	11.880	-0.071	-0.001	11.879	1.431	0.012	9.939	1941.296	16.341	11.880	-0.083	-0.001	11.880
Passenger Vessel	22.227	-7.282	-0.033	22.224	-3.979	-0.018	22.224	-3.623	-0.016	23.124	-903.913	-4.068	22.224	-3.979	-0.018	22.220
Naval I	4.451	-1.344	-0.030	4.450	0.015	0.000	4.450	0.168	0.004	4.830	-379.962	-8.538	4.450	0.015	0.000	4.450
Naval II	4.904	-54.232	-1.118	4.850	-0.037	-0.001	4.850	0.142	0.003	5.274	-424.409	-8.751	4.850	-0.041	-0.001	4.850
Container Vessel	14.975	-74.866	-0.502	14.900	-0.001	0.000	14.898	1.722	0.012	19.061	-4160.818	-27.925	14.900	0.071	0.000	14.900
Supply Vessel	7.492	7.813	0.104	7.500	-0.023	0.000	7.500	0.226	0.003	8.096	-596.476	-7.953	7.500	-0.009	0.000	7.500
	Pos. Avg.:	25.339	0.285	Pos. Avg.:	0.469	0.002	Pos. Avg.:	0.852	0.006	Pos. Avg.:	1053.966	9.580	Pos. Avg.:	0.480	0.002	

Table E.6: VCG obtained from technical incline, Max heel = 10, and Initial heel = 0.5

	Classical			Generalised			Graphical_M			Graphical_G			Polar			Actual
Vessel type	**VCG [m]**	**Error [mm]**	**Error [%]**	**VCG [m]**	**Error [mm]**	**Error [%]**	**VCG [m]**	**Error [mm]**	**Error [%]**	**VCG [m]**	**Error [mm]**	**Error [%]**	**VCG [m]**	**Error [mm]**	**Error [%]**	**VCG [m]**
Fishing Vessel	5.830	20.171	0.345	5.850	-0.060	-0.001	5.850	-0.002	0.000	5.995	-145.296	-2.484	5.850	-0.061	-0.001	5.850
Yacht	3.838	12.338	0.320	3.850	0.000	0.000	3.850	0.072	0.002	4.013	-162.519	-4.221	3.850	-0.001	0.000	3.850
RoPax	13.474	-73.808	-0.551	13.400	0.001	0.000	13.400	0.348	0.003	14.132	-732.316	-5.465	13.400	-0.025	0.000	13.400
Bulk Carrier	11.690	189.836	1.598	11.880	0.102	0.001	11.878	1.662	0.014	11.656	223.752	1.883	11.880	0.088	0.001	11.880
Passenger Vessel	22.317	-96.900	-0.436	22.224	-3.954	-0.018	22.224	-3.533	-0.016	23.091	-871.376	-3.922	22.224	-3.957	-0.018	22.220
Naval I	4.560	-109.825	-2.468	4.450	0.029	0.001	4.450	0.243	0.005	4.818	-368.062	-8.271	4.450	0.027	0.001	4.450
Naval II	5.119	-268.989	-5.546	4.850	-0.013	0.000	4.850	0.244	0.005	5.264	-414.379	-8.544	4.850	-0.011	0.000	4.850
Container Vessel	15.411	-510.878	-3.429	14.900	-0.028	0.000	14.898	1.911	0.013	18.911	-4011.257	-26.921	14.900	0.053	0.000	14.900
Supply Vessel	7.498	1.516	0.020	7.500	-0.004	0.000	7.500	0.265	0.004	8.074	-573.746	-7.650	7.500	0.011	0.000	7.500
	Pos. Avg.:	142.696	1.635	Pos. Avg.:	0.466	0.002	Pos. Avg.:	0.920	0.007	Pos. Avg.:	833.634	7.707	Pos. Avg.:	0.470	0.002	

Table E.7: VCG obtained from technical incline, Max heel = 2, and Initial heel = 1

	Classical			Generalised			Graphical_M			Graphical_G			Polar			Actual
Vessel type	**VCG [m]**	**Error [mm]**	**Error [%]**	**VCG [m]**	**Error [mm]**	**Error [%]**	**VCG [m]**	**Error [mm]**	**Error [%]**	**VCG [m]**	**Error [mm]**	**Error [%]**	**VCG [m]**	**Error [mm]**	**Error [%]**	**VCG [m]**
Fishing Vessel	5.851	-0.709	-0.012	5.850	-0.093	-0.002	5.850	0.143	0.002	6.807	-956.607	-16.352	5.850	-0.094	-0.002	5.850
Yacht	3.848	1.836	0.048	3.850	0.005	0.000	3.850	0.271	0.007	4.923	-1073.395	-27.880	3.850	0.005	0.000	3.850
RoPax	13.341	59.341	0.443	13.400	0.003	0.000	13.399	1.117	0.008	18.024	-4623.775	-34.506	13.400	-0.038	0.000	13.400
Bulk Carrier	11.885	-5.373	-0.045	11.880	-0.117	-0.001	11.874	5.921	0.050	32.961	-21081.338	-177.452	11.880	-0.142	-0.001	11.880
Passenger Vessel	22.227	-6.929	-0.031	22.224	-3.974	-0.018	22.223	-2.559	-0.012	27.914	-5693.740	-25.624	22.224	-3.975	-0.018	22.220
Naval I	4.443	7.224	0.162	4.450	0.005	0.000	4.449	0.606	0.014	6.843	-2392.591	-53.766	4.450	0.005	0.000	4.450
Naval II	4.858	-8.480	-0.175	4.850	-0.051	-0.001	4.849	0.610	0.013	7.507	-2657.199	-54.788	4.850	-0.058	-0.001	4.850
Container Vessel	14.920	-20.327	-0.136	14.900	-0.051	0.000	14.893	6.791	0.046	34.011	-19110.949	-128.261	14.900	0.094	0.001	14.900
Supply Vessel	7.495	4.995	0.067	7.500	-0.036	0.000	7.499	0.958	0.013	11.387	-3886.851	-51.825	7.500	-0.008	0.000	7.500
	Pos. Avg.:	12.801	0.124	Pos. Avg.:	0.482	0.003	Pos. Avg.:	2.108	0.018	Pos. Avg.:	6830.716	63.384	Pos. Avg.:	0.491	0.003	

Table E.8: VCG obtained from technical incline, Max heel = 4, and Initial heel = 1

	Classical			Generalised			Graphical_M			Graphical_G			Polar			Actual
Vessel type	**VCG [m]**	**Error [mm]**	**Error [%]**	**VCG [m]**	**Error [mm]**	**Error [%]**	**VCG [m]**	**Error [mm]**	**Error [%]**	**VCG [m]**	**Error [mm]**	**Error [%]**	**VCG [m]**	**Error [mm]**	**Error [%]**	**VCG [m]**
Fishing Vessel	5.849	1.159	0.020	5.850	-0.083	-0.001	5.850	0.151	0.003	5.928	-78.215	-1.337	5.850	-0.084	-0.001	5.850
Yacht	3.846	4.322	0.112	3.850	0.008	0.000	3.850	0.270	0.007	3.938	-88.435	-2.297	3.850	0.008	0.000	3.850
RoPax	13.353	46.836	0.350	13.400	0.006	0.000	13.399	1.131	0.008	13.753	-353.235	-2.636	13.400	-0.036	0.000	13.400
Bulk Carrier	11.870	9.795	0.082	11.880	-0.078	-0.001	11.874	5.930	0.050	8.058	3821.734	32.169	11.880	-0.102	-0.001	11.880
Passenger Vessel	22.231	-11.480	-0.052	22.224	-3.971	-0.018	22.223	-2.554	-0.011	22.673	-452.831	-2.038	22.224	-3.972	-0.018	22.220
Naval I	4.453	-2.842	-0.064	4.450	0.014	0.000	4.449	0.622	0.014	4.631	-180.810	-4.063	4.450	0.014	0.000	4.450
Naval II	4.890	-39.680	-0.818	4.850	-0.039	-0.001	4.849	0.661	0.014	5.014	-164.166	-3.385	4.850	-0.046	-0.001	4.850
Container Vessel	14.967	-67.339	-0.452	14.900	-0.068	0.000	14.893	6.806	0.046	16.995	-2094.970	-14.060	14.900	0.078	0.001	14.900
Supply Vessel	7.495	4.748	0.063	7.500	-0.033	0.000	7.499	0.960	0.013	7.809	-309.494	-4.127	7.500	-0.005	0.000	7.500
	Pos. Avg.:	20.911	0.224	Pos. Avg.:	0.478	0.002	Pos. Avg.:	2.121	0.018	Pos. Avg.:	838.210	7.346	Pos. Avg.:	0.483	0.002	

Table E.9: VCG obtained from technical incline, Max heel = 10, and Initial heel = 1

	Classical			Generalised			Graphical_M			Graphical_G			Polar			Actual
Vessel type	**VCG [m]**	**Error [mm]**	**Error [%]**	**VCG [m]**	**Error [mm]**	**Error [%]**	**VCG [m]**	**Error [mm]**	**Error [%]**	**VCG [m]**	**Error [mm]**	**Error [%]**	**VCG [m]**	**Error [mm]**	**Error [%]**	**VCG [m]**
Fishing Vessel	5.833	17.350	0.297	5.850	-0.059	-0.001	5.850	0.164	0.003	5.928	-77.783	-1.330	5.850	-0.060	-0.001	5.850
Yacht	3.839	10.577	0.275	3.850	0.003	0.000	3.850	0.273	0.007	3.934	-84.368	-2.191	3.850	0.000	0.000	3.850
RoPax	13.468	-67.889	-0.507	13.400	0.024	0.000	13.399	1.315	0.010	13.732	-332.241	-2.479	13.400	-0.026	0.000	13.400
Bulk Carrier	11.723	157.447	1.325	11.880	0.112	0.001	11.874	6.052	0.051	10.822	1057.719	8.903	11.880	0.084	0.001	11.880
Passenger Vessel	22.314	-93.633	-0.421	22.224	-3.950	-0.018	22.222	-2.379	-0.011	22.647	-427.495	-1.924	22.224	-3.958	-0.018	22.220
Naval I	4.552	-102.342	-2.300	4.450	0.031	0.001	4.449	0.809	0.018	4.609	-159.455	-3.583	4.450	0.027	0.001	4.450
Naval II	5.091	-241.347	-4.976	4.850	-0.019	0.000	4.849	0.925	0.019	4.998	-148.188	-3.055	4.850	-0.015	0.000	4.850
Container Vessel	15.378	-477.870	-3.207	14.900	-0.101	-0.001	14.893	7.285	0.049	16.916	-2015.797	-13.529	14.900	0.053	0.000	14.900
Supply Vessel	7.502	-1.733	-0.023	7.500	-0.018	0.000	7.499	1.001	0.013	7.802	-301.965	-4.026	7.500	0.010	0.000	7.500
	Pos. Avg.:	130.021	1.481	Pos. Avg.:	0.480	0.002	Pos. Avg.:	2.245	0.020	Pos. Avg.:	511.668	4.558	Pos. Avg.:	0.470	0.002	

Table E.10: TCG obtained from technical incline, Max heel = 2, and Initial heel = 0

	Classical			Generalised			Polar			Actual
Vessel type	**TCG [m]**	**Error [mm]**	**Error [%]**	**TCG [m]**	**Error [mm]**	**Error [%]**	**TCG [m]**	**Error [mm]**	**Error [%]**	**TCG [m]**
Fishing Vessel	0.000	0.041	0.001	0.000	0.042	0.001	0.000	0.003	0.000	0.000
Yacht	0.000	0.002	0.000	0.000	0.004	0.000	0.000	0.000	0.000	0.000
RoPax	0.002	0.009	0.000	0.000	2.356	0.018	0.002	0.002	0.000	0.002
Bulk Carrier	0.002	-0.563	-0.003	0.000	1.390	0.009	0.001	0.002	0.000	0.001
Passenger Vessel	0.000	0.025	0.000	0.000	0.022	0.000	0.000	-0.002	0.000	0.000
Naval I	0.000	0.000	0.000	0.000	0.000	0.000	0.000	0.000	0.000	0.000
Naval II	0.000	0.371	0.006	0.000	0.371	0.006	0.000	0.000	0.000	0.000
Container Vessel	-0.009	0.252	0.001	0.000	-8.285	-0.034	-0.008	0.001	0.000	-0.008
Supply Vessel	-0.001	-0.524	-0.005	0.000	-1.599	-0.016	-0.002	0.000	0.000	-0.002
	Pos. Avg.:	0.198	0.002	Pos. Avg.:	1.563	0.009	Pos. Avg.:	0.001	0.000	

Table E.11: TCG obtained from technical incline, Max heel = 4, and Initial heel = 0

	Classical			Generalised			Polar			Actual
Vessel type	**TCG [m]**	**Error [mm]**	**Error [%]**	**TCG [m]**	**Error [mm]**	**Error [%]**	**TCG [m]**	**Error [mm]**	**Error [%]**	**TCG [m]**
Fishing Vessel	0.000	0.041	0.001	0.000	0.040	0.001	0.000	0.003	0.000	0.000
Yacht	0.000	0.002	0.000	0.000	0.004	0.000	0.000	0.000	0.000	0.000
RoPax	0.002	0.009	0.000	0.000	2.356	0.018	0.002	0.002	0.000	0.002
Bulk Carrier	0.002	-0.563	-0.003	0.000	1.404	0.009	0.001	0.002	0.000	0.001
Passenger Vessel	0.000	0.025	0.000	0.000	0.022	0.000	0.000	-0.002	0.000	0.000
Naval I	0.000	0.000	0.000	0.000	0.000	0.000	0.000	0.000	0.000	0.000
Naval II	0.000	0.371	0.006	0.000	0.376	0.006	0.000	0.000	0.000	0.000
Container Vessel	-0.009	0.252	0.001	0.000	-8.291	-0.034	-0.008	0.001	0.000	-0.008
Supply Vessel	-0.001	-0.524	-0.005	0.000	-1.599	-0.016	-0.002	0.000	0.000	-0.002
	Pos. Avg.:	0.198	0.002	Pos. Avg.:	1.566	0.009	Pos. Avg.:	0.001	0.000	

Table E.12: TCG obtained from technical incline, Max heel = 10, and Initial heel = 0

	Classical			Generalised			Polar			Actual
Vessel type	**TCG [m]**	**Error [mm]**	**Error [%]**	**TCG [m]**	**Error [mm]**	**Error [%]**	**TCG [m]**	**Error [mm]**	**Error [%]**	**TCG [m]**
Fishing Vessel	0.000	0.041	0.001	0.000	0.023	0.000	0.000	0.003	0.000	0.000
Yacht	0.000	0.002	0.000	0.000	0.018	0.000	0.000	0.000	0.000	0.000
RoPax	0.002	0.009	0.000	0.000	2.362	0.018	0.002	0.002	0.000	0.002
Bulk Carrier	0.002	-0.563	-0.003	0.000	1.562	0.010	0.001	0.002	0.000	0.001
Passenger Vessel	0.000	0.025	0.000	0.000	0.058	0.000	0.000	-0.002	0.000	0.000
Naval I	0.000	0.000	0.000	0.000	0.025	0.000	0.000	0.000	0.000	0.000
Naval II	0.000	0.371	0.006	0.000	0.375	0.006	0.000	0.000	0.000	0.000
Container Vessel	-0.009	0.252	0.001	0.000	-8.053	-0.033	-0.008	0.001	0.000	-0.008
Supply Vessel	-0.001	-0.524	-0.005	0.000	-1.597	-0.016	-0.002	0.000	0.000	-0.002
	Pos. Avg.:	0.198	0.002	Pos. Avg.:	1.564	0.010	Pos. Avg.:	0.001	0.000	

Table E.13: TCG obtained from technical incline, Max heel = 2, and Initial heel = 0.5

	Classical			Generalised			Polar			Actual
Vessel type	**TCG [m]**	**Error [mm]**	**Error [%]**	**TCG [m]**	**Error [mm]**	**Error [%]**	**TCG [m]**	**Error [mm]**	**Error [%]**	**TCG [m]**
Fishing Vessel	0.007	0.035	0.001	0.007	0.042	0.001	0.007	0.003	0.000	0.007
Yacht	0.008	-0.010	0.000	0.008	0.004	0.000	0.008	0.000	0.000	0.008
RoPax	0.034	0.054	0.000	0.032	2.356	0.018	0.034	0.002	0.000	0.034
Bulk Carrier	0.175	-0.613	-0.004	0.173	1.389	0.009	0.174	0.002	0.000	0.174
Passenger Vessel	0.041	0.045	0.000	0.041	0.022	0.000	0.041	-0.002	0.000	0.041
Naval I	0.017	0.065	0.001	0.017	0.000	0.000	0.017	0.000	0.000	0.017
Naval II	0.019	0.391	0.007	0.019	0.371	0.006	0.019	0.000	0.000	0.019
Container Vessel	0.187	0.393	0.002	0.196	-8.284	-0.034	0.188	0.001	0.000	0.188
Supply Vessel	0.027	-0.523	-0.005	0.028	-1.599	-0.016	0.027	0.000	0.000	0.027
	Pos. Avg.:	0.237	0.002	Pos. Avg.:	1.563	0.009	Pos. Avg.:	0.001	0.000	

Table E.14: TCG obtained from technical incline, Max heel = 4, and Initial heel = 0.5

	Classical			Generalised			Polar			Actual
Vessel type	**TCG [m]**	**Error [mm]**	**Error [%]**	**TCG [m]**	**Error [mm]**	**Error [%]**	**TCG [m]**	**Error [mm]**	**Error [%]**	**TCG [m]**
Fishing Vessel	0.007	0.015	0.000	0.007	0.041	0.001	0.007	0.003	0.000	0.007
Yacht	0.008	-0.037	-0.001	0.008	0.006	0.000	0.008	0.000	0.000	0.008
RoPax	0.034	0.182	0.001	0.032	2.357	0.018	0.034	0.002	0.000	0.034
Bulk Carrier	0.175	-0.798	-0.005	0.173	1.397	0.009	0.174	0.001	0.000	0.174
Passenger Vessel	0.040	0.082	0.000	0.041	0.026	0.000	0.041	-0.002	0.000	0.041
Naval I	0.017	0.151	0.003	0.017	0.002	0.000	0.017	0.000	0.000	0.017
Naval II	0.018	0.779	0.013	0.019	0.367	0.006	0.019	0.000	0.000	0.019
Container Vessel	0.187	0.885	0.004	0.196	-8.287	-0.034	0.188	0.001	0.000	0.188
Supply Vessel	0.027	-0.524	-0.005	0.028	-1.599	-0.016	0.027	0.000	0.000	0.027
	Pos. Avg.:	0.384	0.004	Pos. Avg.:	1.565	0.009	Pos. Avg.:	0.001	0.000	

Table E.15: TCG obtained from technical incline, Max heel = 10, and Initial heel = 0.5

	Classical			Generalised			Polar			Actual
Vessel type	**TCG [m]**	**Error [mm]**	**Error [%]**	**TCG [m]**	**Error [mm]**	**Error [%]**	**TCG [m]**	**Error [mm]**	**Error [%]**	**TCG [m]**
Fishing Vessel	0.007	-0.138	-0.002	0.007	0.029	0.000	0.007	0.003	0.000	0.007
Yacht	0.008	-0.092	-0.002	0.008	0.103	0.003	0.008	0.000	0.000	0.008
RoPax	0.033	1.259	0.010	0.032	2.415	0.019	0.034	0.002	0.000	0.034
Bulk Carrier	0.177	-2.245	-0.014	0.173	1.601	0.010	0.174	0.000	0.000	0.174
Passenger Vessel	0.040	0.864	0.004	0.040	0.317	0.002	0.041	-0.003	0.000	0.041
Naval I	0.016	1.098	0.021	0.017	0.156	0.003	0.017	0.000	0.000	0.017
Naval II	0.017	2.653	0.044	0.019	-0.122	-0.002	0.019	0.000	0.000	0.019
Container Vessel	0.183	4.690	0.019	0.196	-8.123	-0.033	0.188	0.001	0.000	0.188
Supply Vessel	0.027	-0.469	-0.005	0.028	-1.565	-0.016	0.027	0.000	0.000	0.027
	Pos. Avg.:	1.501	0.013	Pos. Avg.:	1.603	0.010	Pos. Avg.:	0.001	0.000	

Table E.16: TCG obtained from technical incline, Max heel = 2, and Initial heel = 1

	Classical			Generalised			Polar			Actual
Vessel type	**TCG [m]**	**Error [mm]**	**Error [%]**	**TCG [m]**	**Error [mm]**	**Error [%]**	**TCG [m]**	**Error [mm]**	**Error [%]**	**TCG [m]**
Fishing Vessel	0.014	0.030	0.000	0.014	0.042	0.001	0.014	0.003	0.000	0.014
Yacht	0.015	-0.021	-0.001	0.015	0.004	0.000	0.015	0.000	0.000	0.015
RoPax	0.066	0.119	0.001	0.064	2.356	0.018	0.066	0.002	0.000	0.066
Bulk Carrier	0.348	-0.653	-0.004	0.346	1.389	0.008	0.348	0.002	0.000	0.348
Passenger Vessel	0.081	0.070	0.000	0.081	0.023	0.000	0.081	-0.002	0.000	0.081
Naval I	0.034	0.114	0.002	0.034	0.000	0.000	0.034	0.000	0.000	0.034
Naval II	0.038	0.553	0.009	0.038	0.371	0.006	0.038	0.000	0.000	0.038
Container Vessel	0.383	0.615	0.003	0.392	-8.284	-0.034	0.383	0.001	0.000	0.383
Supply Vessel	0.056	-0.515	-0.005	0.057	-1.599	-0.016	0.055	0.000	0.000	0.055
	Pos. Avg.:	0.299	0.003	Pos. Avg.:	1.563	0.009	Pos. Avg.:	0.001	0.000	

Table E.17: TCG obtained from technical incline, Max heel = 4, and Initial heel = 1

	Classical			Generalised			Polar			Actual
Vessel type	**TCG [m]**	**Error [mm]**	**Error [%]**	**TCG [m]**	**Error [mm]**	**Error [%]**	**TCG [m]**	**Error [mm]**	**Error [%]**	**TCG [m]**
Fishing Vessel	0.014	-0.003	0.000	0.014	0.042	0.001	0.014	0.003	0.000	0.014
Yacht	0.015	-0.065	-0.002	0.015	0.004	0.000	0.015	0.000	0.000	0.015
RoPax	0.066	0.337	0.003	0.064	2.356	0.018	0.066	0.002	0.000	0.066
Bulk Carrier	0.348	-0.918	-0.006	0.346	1.389	0.008	0.348	0.001	0.000	0.348
Passenger Vessel	0.081	0.150	0.001	0.081	0.021	0.000	0.081	-0.003	0.000	0.081
Naval I	0.034	0.290	0.005	0.034	-0.001	0.000	0.034	0.000	0.000	0.034
Naval II	0.037	1.098	0.018	0.038	0.374	0.006	0.038	0.000	0.000	0.038
Container Vessel	0.382	1.436	0.006	0.392	-8.285	-0.034	0.383	0.001	0.000	0.383
Supply Vessel	0.056	-0.511	-0.005	0.057	-1.599	-0.016	0.055	0.000	0.000	0.055
	Pos. Avg.:	0.534	0.005	Pos. Avg.:	1.563	0.009	Pos. Avg.:	0.001	0.000	

Table E.18: TCG obtained from technical incline, Max heel = 10, and Initial heel = 1

	Classical			Generalised			Polar			Actual
Vessel type	**TCG [m]**	**Error [mm]**	**Error [%]**	**TCG [m]**	**Error [mm]**	**Error [%]**	**TCG [m]**	**Error [mm]**	**Error [%]**	**TCG [m]**
Fishing Vessel	0.014	-0.286	-0.005	0.014	0.033	0.001	0.014	0.003	0.000	0.014
Yacht	0.015	-0.174	-0.005	0.015	0.135	0.004	0.015	0.000	0.000	0.015
RoPax	0.064	2.340	0.018	0.064	2.429	0.019	0.066	0.001	0.000	0.066
Bulk Carrier	0.351	-3.495	-0.021	0.346	1.598	0.010	0.348	-0.002	0.000	0.348
Passenger Vessel	0.080	1.584	0.008	0.081	0.399	0.002	0.081	-0.003	0.000	0.081
Naval I	0.032	2.026	0.038	0.034	0.175	0.003	0.034	0.000	0.000	0.034
Naval II	0.033	4.618	0.076	0.038	-0.174	-0.003	0.038	-0.001	0.000	0.038
Container Vessel	0.375	8.602	0.035	0.392	-8.181	-0.033	0.383	0.002	0.000	0.383
Supply Vessel	0.056	-0.398	-0.004	0.057	-1.551	-0.016	0.055	0.000	0.000	0.055
	Pos. Avg.:	2.614	0.023	Pos. Avg.:	1.631	0.010	Pos. Avg.:	0.001	0.000	